

*Dissertation*  
*On*  
**THERMAL PERFORMANCE OF LOW FLUX SOLAR COLLECTORS  
USING  $\text{Al}_2\text{O}_3$ -  $\text{H}_2\text{O}$  BASED NANOFLUIDS**

*Submitted in partial fulfillment of the requirements for the award of degree of*

**Master of Engineering**  
**IN**  
**Thermal Engineering**

*Submitted by*  
**Vivek Verma**

**Roll No: 801083028**

**Under the guidance of**

**Mr. Kundan Lal**  
**Assistant Professor**  
**Mechanical Engineering Department**  
**Thapar University, Patiala**



**MECHANICAL ENGINEERING DEPARTMENT**  
**THAPAR UNIVERSITY**  
**PATIALA – 147004**

## DECLARATION

---

I, "Vivek verma", hereby certify that the work which is being presented in this thesis entitled "Thermal performance of low flux solar collector using  $Al_2O_3$ -  $H_2O$  based nanofluid" by me in partial fulfillment of the requirements for the award of degree of Master of Engineering in Thermal Engineering from Thapar University, Patiala, is an authentic record of my own work carried out under the supervision of "Mr. Kundan lal, Assistant Professor, MED".

The matter embodied in this thesis has not been submitted in any other University / Institute for the award of any other degree.

Date: 6/07/2012

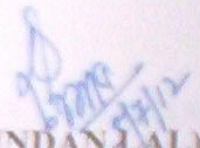


(VIVEK VERMA)

Reg. No. 801083028

This is to certify that the above statement made by the student concerned is correct to the best of my knowledge and belief.

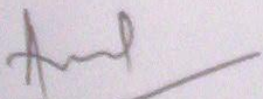
Date: 6/07/2012



(Mr. KUNDAN LAL)

Assistant Professor  
Mechanical Engineering Department  
Thapar University, Patiala

*Countersigned by:*



(Dr. AJAY BATISH)

Professor and Head  
Mechanical Engineering Department  
Thapar University,  
Patiala - 147004



(Dr. S.K. MOHAPATRA)

Dean of Academic Affairs  
Thapar University  
Patiala - 147004

## ACKNOWLEDGEMENT

---

I express my sincere gratitude to **Mr. Kundan Lal**, *Assistant Professor*, Mechanical Engineering Department Thapar University, Patiala for his valuable guidance, constructive suggestions and constant encouragement in the nurturing work.

I also pay my thanks to **Dr. S.S.Mallick**, *Assistant Prof. MED* for their valuable directions and advices. I am grateful to **Dr. Ajay Batish**, *Prof. & Head, MED* for providing the facilities for the completion of the work.

I also express my thanks to the faculty and staff of **Mechanical Engineering Department Thapar University, Patiala**, for their help, inspiration and moral support. Above all, I express my indebtedness to the “*ALMIGHTY*” for his blessings and kindness.

**VIVEK VERMA**

**Reg. No. 801083028**

## ABSTRACT

---

Due to the growing demand of energy and lesser availability of fossil fuels, it shifts our concern towards Renewable energy sources. From all of the sources available to us solar energy is the best option with minimum environmental impact. But the problem lies in efficiently collecting and converting this energy into something useful form. The present study has been carried out to increase the efficiency of the solar collector by using new type of solar collector(DASC-Direct absorption Solar collector) and different class of fluids called(Nanofluids). In conventional type of flat plate solar collectors we get three resistances whereas in DASC these three resistances are reduced to one. In the present work we have evaluated the collector efficiency using water and  $\text{Al}_2\text{O}_3$  nanofluid with volume concentration .005% and .05% at different mass flow rates 60,80 and 100ml/hr. Also the variation of temperature difference with time is also plotted. By performing the experiment it has been found that the efficiency of the flat plate DASC using  $\text{Al}_2\text{O}_3$  nanofluid is 3-4% more than using the water. Whereas if we compare two concentrations of Nanofluids, at higher concentrations the tendency of the nanoparticles to settle down is higher. By varying the mass flow rate and varying the volume concentration of nanoparticles in nanofluids the variation in collector efficiency and temperature difference are studied. At last the comparison of efficiency graphs of  $\text{Al}_2\text{O}_3$  and  $\text{CuO}$  Nanofluids at same concentration are done.

# INDEX

| <b>CONTENTS</b>                              | <b>Page No.</b> |
|--|-----------------|
| <b>DECLARATION</b>                           | ii              |
| <b>ACKNOWLEDGEMENT</b>                       | iii             |
| <b>ABSTRACT</b>                              | iv              |
| <b>Chapter 1: INTRODUCTION</b>               | 1               |
| 1.1 Solar Energy                             | 2               |
| 1.1.1 Solar thermal conversion               | 2               |
| 1.1.2 earth- sun distance                    | 3               |
| 1.1.3 solar constant                         | 3               |
| 1.2 Solar Collectors                         | 3               |
| 1.2.1 Non-concentrating type solar collector | 3               |
| 1.2.2 Direct absorption solar collector      | 5               |
| 1.3 Nano-Fluids                              | 6               |
| 1.3.1 Preparation methods for nanoparticles  | 7               |
| 1.3.2 Preparation methods for nanofluids     | 7               |
| 1.3.2.1 two step method                      | 7               |
| 1.3.2.2 single step method                   | 8               |
| <b>Chapter 2: OBJECTIVE</b>                  | 9               |
| 2.1 Objective                                | 10              |
| <b>Chapter 3: LITERATURE REVIEW</b>          | 21              |
| 3.1 Literature review                        | 22              |

|   |    |
|---|----|
| <b>Chapter 4: METHODOLOGY</b>                             | 19 |
| 4.1 ASHRAE Standards 93-77                                | 19 |
| 4.2 Experimental set - up                                 | 20 |
| 4.3 Preparation of nanofluids                             | 23 |
| 4.4 Instruments   | 26 |
| <b>Chapter 5: RESULTS AND DISCUSSION</b>                  | 30 |
| 5.1 Solar collector instantaneous efficiency calculations | 30 |
| <b>Chapter 6 : CONCLUSION AND FUTURE SCOPE</b>            | 51 |
| <b>REFERENCES</b>   | 52 |
| <b>ANNEXURE</b>   | 54 |

## LIST OF FIGURES

---

|   |         |
|---|---------|
| Figure 1.1: Pictorial view of Flat Plate Collector  | Page 3  |
| Figure 1.2: Exploded view of a flat plate collector   | Page 3  |
| Figure 1.3a: DASC-Conventional Collector  | Page 5  |
| Figure 1.3b: DASC Collector   | Page 5  |
| Figure 2.1: Variation of collector efficiency with volume fraction                            | Page 10 |
| Figure 2.2: Variation of stagnation temp. diff. with volume fraction                          | Page 11 |
| Figure 2.3: Collector efficiency as a function of diameter and vol. fraction                  | Page 11 |
| Figure 2.4: Reflective dish and machined parts with inlet ports                               | Page 12 |
| Figure 2.5: Variation of receiver efficiency with solar conc. ratio                           | Page 13 |
| Figure 2.6: Schematic diagram of the collector  | Page 15 |
| Figure 2.7: Variation of collector efficiency with temp diff                                  | Page 16 |
| Figure 2.8: Effect of Nanofluids on the efficiency of collector                               | Page 17 |
| Figure 4.1: 3D model of Experimental Set – up   | Page 21 |
| Figure 4.2: Exploded 3D view of Collector   | Page 22 |
| Figure 4.3: Dimensions of Solar collector   | Page 23 |
| Figure 4.4: Actual view of Solar Collector  | Page 23 |
| Figure 4.5: Oscar Ultra sonicator(probe type)   | Page 26 |
| Figure 4.6a: Al <sub>2</sub> O <sub>3</sub> -H <sub>2</sub> O nanofluid with .005% vol. conc. | Page 27 |
| Figure 4.6b: Al <sub>2</sub> O <sub>3</sub> -H <sub>2</sub> O nanofluid with .05% vol. conc.  | Page 27 |
| Figure 4.7: Parts of pyranometer  | Page 28 |
| Figure 4.8: Kipp and Zonen Pyranometer  | Page 28 |
| Figure 4.9a: Infusion set with storage Bottle   | Page 29 |
| Figure 4.9b: Flow control mechanism   | Page 29 |
| Figure 5.1: Variation of Solar Irradiation  | Page 32 |
| Figure 5.2: Plot (Temp. Diff. vs Time) for water  | Page 34 |
| Figure 5.3: Plot (Efficiency vs Time) for water   | Page 35 |
| Figure 5.4: Plot (Temp. Diff. vs Time) for Al <sub>2</sub> O <sub>3</sub> nanofluid (0.05%)   | Page 37 |
| Figure 5.5: Plot (Efficiency vs Time) for Al <sub>2</sub> O <sub>3</sub> nanofluid (0.05%)    | Page 38 |
| Figure 5.6: Plot (Temp. Diff. vs Time) for Al <sub>2</sub> O <sub>3</sub> nanofluid (0.005%)  | Page 40 |

Figure 5.7: Plot (Efficiency vs Time) for Al<sub>2</sub>O<sub>3</sub> nanofluid (0.005%) Page 41

**Performance Comparison Charts:-**

**(i) Water vs Al<sub>2</sub>O<sub>3</sub> nanofluid (volume fraction – 0.05%)**

Figure 5.8: Plot (Temp. Diff. vs Time) for flow rate - 60 ml/hr Page 42

Figure 5.9: Plot (Temp. Diff. vs Time) for flow rate - 80 ml/hr Page 42

Figure 5.10: Plot (Temp. Diff. vs Time) for flow rate - 100 ml/hr Page 43

Figure 5.11: Plot (Efficiency vs Time) for flow rate – 60ml/hr Page 43

Figure 5.12: Plot (Efficiency vs Time) for flow rate – 80ml/hr Page 44

Figure 5.13: Plot (Efficiency vs Time) for flow rate – 100ml/hr Page 44

**(ii) Water vs Al<sub>2</sub>O<sub>3</sub> nanofluid (volume fraction – 0.005%)**

Figure 5.14: Plot (Temp. Diff. vs Time) for flow rate - 60 ml/hr Page 45

Figure 5.15: Plot (Temp. Diff. vs Time) for flow rate - 80 ml/hr Page 45

Figure 5.16: Plot (Temp. Diff. vs Time) for flow rate - 100 ml/hr Page 46

Figure 5.17: Plot (Efficiency vs Time) for flow rate – 60ml/hr Page 46

Figure 5.18: Plot (Efficiency vs Time) for flow rate – 80ml/hr Page 47

Figure 5.19: Plot (Efficiency vs Time) for flow rate – 100ml/hr Page 47

**(iii) Al<sub>2</sub>O<sub>3</sub> nanofluid (volume fraction – 0.05%) vs (Volume fraction – 0.005%)**

Figure 5.20: Plot (Temp. Diff. vs Time) for flow rate - 60 ml/hr Page 48

Figure 5.21: Plot (Temp. Diff. vs Time) for flow rate - 80 ml/hr Page 48

Figure 5.22: Plot (Temp. Diff. vs Time) for flow rate - 100 ml/hr Page 49

Figure 5.23: Plot (Efficiency vs Time) for flow rate – 60ml/hr Page 50

Figure 5.24: Plot (Efficiency vs Time) for flow rate – 80ml/hr Page 50

Figure 5.25: Plot (Efficiency vs Time) for flow rate – 100ml/hr Page 51

## LIST OF TABLES

---

|   |         |
|---|---------|
| Table 4.1: Weight of nanoparticles for different concentration  | Page 25 |
| Table 5.1: Solar radiation readings from pyranometer  | Page 32 |
| Table 5.2: Total Solar radiation incident on collector Box  | Page 33 |
| Table 5.3: Mass flow rate for water   | Page 33 |
| Table 5.4: Temperature readings for water   | Page 34 |
| Table 5.5: Efficiency of collector using water  | Page 35 |
| Table 5.6: Mass flow rate for Al <sub>2</sub> O <sub>3</sub> nanofluid ( $\phi = 0.05\%$ )              | Page 36 |
| Table 5.7: Temperature readings for Al <sub>2</sub> O <sub>3</sub> nanofluid ( $\phi = 0.05\%$ )        | Page 36 |
| Table 5.8: Efficiency of collector using Al <sub>2</sub> O <sub>3</sub> nanofluid ( $\phi = 0.05\%$ )   | Page 37 |
| Table 5.9: Mass flow rate for Al <sub>2</sub> O <sub>3</sub> nanofluid ( $\phi = 0.005\%$ )             | Page 39 |
| Table 5.10: Temperature readings for Al <sub>2</sub> O <sub>3</sub> nanofluid ( $\phi = 0.005\%$ )      | Page 39 |
| Table 5.11: Efficiency of collector using Al <sub>2</sub> O <sub>3</sub> nanofluid ( $\phi = 0.005\%$ ) | Page 40 |

## ABBREVIATIONS

---

### Symbols

|        |   |
|--------|---|
| $K$    | Thermal Conductivity                            |
| $\phi$ | % of Volume Fraction                            |
| $n$    | Shape factor                                    |
| $m$    | mass flow rate                                  |
| $\eta$ | Collector Efficiency                            |
| $C$    | Specific Heat                                   |
| $T$    | Temperature                                     |
| $G_T$  | Solar Irradiation                               |
| $A$    | Solar Collector Area                            |
| $V$    | Volume  |
| $v$    | Volume flow rate                                |
| $W$    | Weight  |
| $\rho$ | Density   |
| $C_r$  | Correction Factor                               |
| $Q_a$  | Heat absorbed by the solar collector            |
| $Q_i$  | Total Av. Solar Radiation fall on the collector |

### Subscripts:

|     |                   |
|-----|-------------------|
| eff | Nanofluid         |
| f   | Base Fluid        |
| P   | Nanoparticle      |
| 1   | Initial Condition |
| 2   | Final Condition   |

### INTRODUCTION

#### 1.1 Solar Energy

Energy is the prime agent in the generation of wealth and a significant factor in economic development. Limited availability of fossil resources and environmental problems associated with them have emphasized the need for new sustainable energy supply options that use renewable energies. Solar energy is one of the best sources of renewable energy with minimal environmental impact. As the primary energy sources are depleting continuously, solar energy draws attention of researchers throughout the world. Everyday sun radiates enormous amount of energy known as solar energy. The hourly solar flux incident on the earth's surface is greater than all of human consumption of energy in a year[1]. So, the problem lies in efficiently collecting and converting this energy into something useful form. The conversion of solar thermal energy into more usable form is done by solar collectors. A solar collector is a device which transfers the collected solar energy to a fluid passing in contact with it, so it is always a matter of investigation to know that how efficiently solar collectors are converting solar energy into thermal energy.

The sun is an excellent source of radiant energy, and is the world's most abundant source of energy. It emits electromagnetic radiation with an average irradiance of  $1353 \text{ W/m}^2$  on the earth's surface. The solar radiation incident on the earth's surface is comprised of two types of radiations – beam and diffuse, ranging in the wavelengths from the ultraviolet to the infrared (300 to 200 nm). To put this into perspective, if the energy produced by 25 acres of the surface of the sun were harvested, there would be enough energy to supply the current energy demand of the world.[2]. When dealing with solar energy, there are two basic choices. The first is photovoltaics, which is direct energy conversion that converts solar radiation to electricity. The second is solar thermal, in which the solar radiation is used to provide heat to a thermodynamic system, thus creating mechanical energy that can be converted to electricity. In commercially available photovoltaic systems, efficiencies are on the order of 10 to 15 percent, where in a solar thermal system, efficiencies as high as 30 percent are achievable [3]. This work focuses on the electric power generation of a flat plate solar collector using nanofluids.

### **1.1.1 Solar thermal conversion**

The basic principle of solar thermal collection is that when solar radiation is incident on a surface (such as that of a black-body), part of this radiation is absorbed, thus increasing the temperature of the surface. As the temperature of the body increases, the surface loses heat at an increasing rate to the surroundings. Steady-state is reached when the rate of the solar heat gain is balanced by the rate of heat loss to the ambient surroundings

### **1.1.2 Earth-sun distance[4]**

The earth has a diameter of  $12.7 \times 10^3$  km, which is approximately 110 times less than the sun's diameter. The earth's orbit's eccentricity is very small, about 0.0167, which causes the elliptical path to be nearly circular. The average earth-sun distance of  $14.9 \times 10^7$  km is defined as the Astronomical Unit (AU), which is used for calculating distances within the solar system.

### **1.1.3 Solar constant**

Solar radiation is a general term for the electromagnetic radiation emitted by the sun. The amount of radiation intercepted by the outer limits of the earth's atmosphere is nearly constant. The varying solar energy output should be referred to as the total solar irradiance (TSI), whereas the long term average of TSI is commonly known as the solar constant (*ISC*).

In order to convert solar energy into something useful form can be carried with the help of solar collectors.

## **1.2 Solar Collectors**

Solar collectors can be classified broadly into two types:

- 1) Non-concentrating type solar collector.
- 2) Concentrating or Focusing type solar collector.

### **1.2.1 Non-concentrating type solar collector**

When no optical concentration is done, the device in which the collection is achieved is called a flat plate collector. The absorber and collector area in flat plate solar collectors is numerically the same. The flat plate collector is most commonly used and most important type of solar collector because it is simple in design, has no moving parts and requires less maintenance. It can be used for a variety of applications in which temperatures ranging from

30<sup>0</sup>C to about 90<sup>0</sup>C. Flat plate collectors can collect both beam and diffused solar radiations ,they are also effective on cloudy days where there is no direct radiation. A flat plate collector consists of a insulated box containing a dark coloured absorber plate, the energy receiver with one or more translucent glazings. Absorber plates are typically made out of metal due to its high thermal conductivity and painted with special selective surface coatings in order to absorb and transfer heat better. Figure 1.1 shows the typical components of a classic flat - plate collector. A heat-conducting fluid, usually water, glycol, or air, passes through pipes attached to the absorber plate. As the fluid flows through the pipes, its temperature increases. This is the energy to be utilized for productive activities (e.g., power generation). The amount of the energy taken by the working fluid corresponds to a fraction of the useful energy collected after the heat losses.

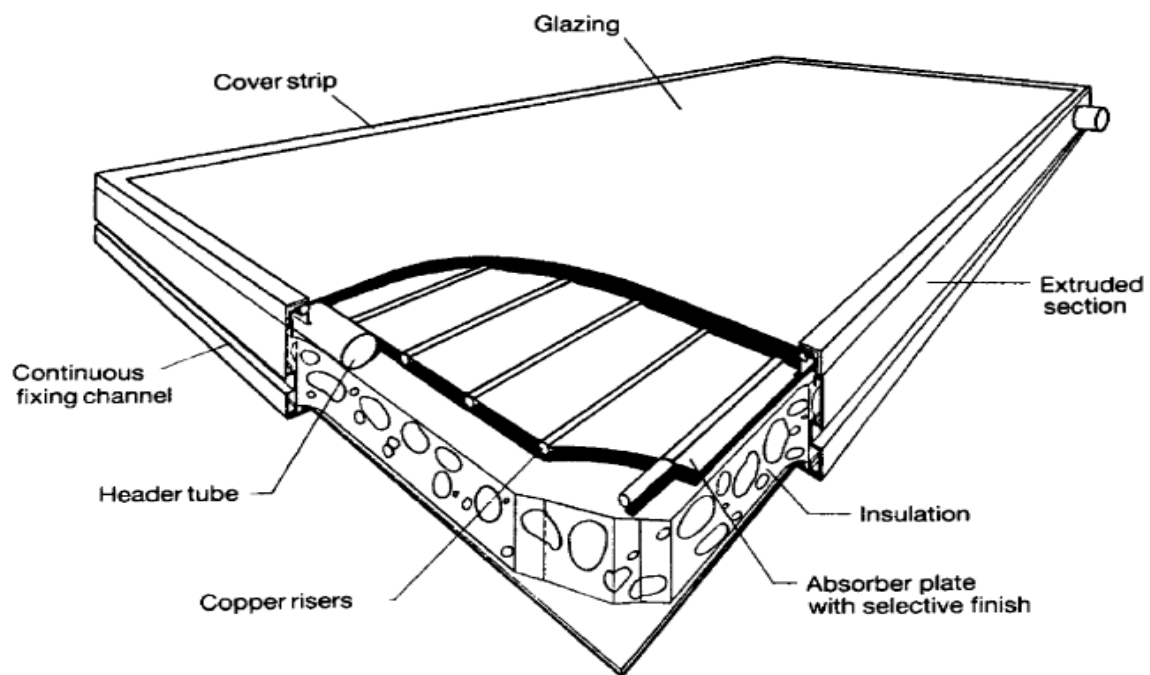


Fig.1.1 Pictorial view of Flat plate collector

A flat plate collector generally consists of the following components as shown in the Fig1.2

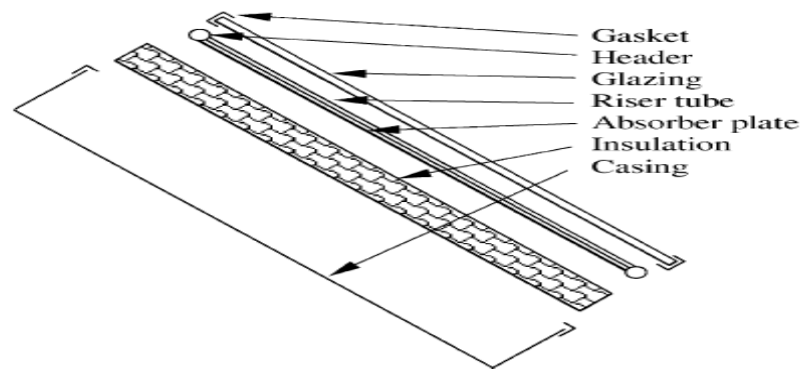


Fig.1.2 Exploded view of a flat-plate collector

Glazing : One or more sheets of glass or other radiation-transmitting material.

Tubes or Passages: To conduct or direct the heat transfer fluid from the inlet to the outlet.

Absorber plates: Flat, corrugated or grooved plates to which tubes, passages are attached.

Insulation: To minimize the heat losses from the back and sides of the collector.

Container or Casing: To surround the above mentioned components and keep them free from dust, moisture, etc.

In conventional type of solar collectors the solar radiations fall over the absorber plate which absorbs the solar radiations and convert it into heat, this heat is then conducted from the absorber plate to the tubes carrying the fluids, after conduction the heat is convected to the working fluid , due to the involvement of three resistances between solar radiations and working fluid the losses are more. In order to reduce the conduction and convection losses from the collector we have to reduce these three resistances. In order to increase the collection efficiency of the collector the solar radiations are directly allowed to fall over the moving fluid, and these type of collectors are known as Direct Absorption Solar Collector. This type of collectors were first introduced in 1970's but due to low absorption properties of working fluids they failed. The absorption properties of the fluids generally used in solar collectors are very poor which in turn limits the efficiency of the solar collector.

### 1.2.2 Direct absorption solar collector[5]

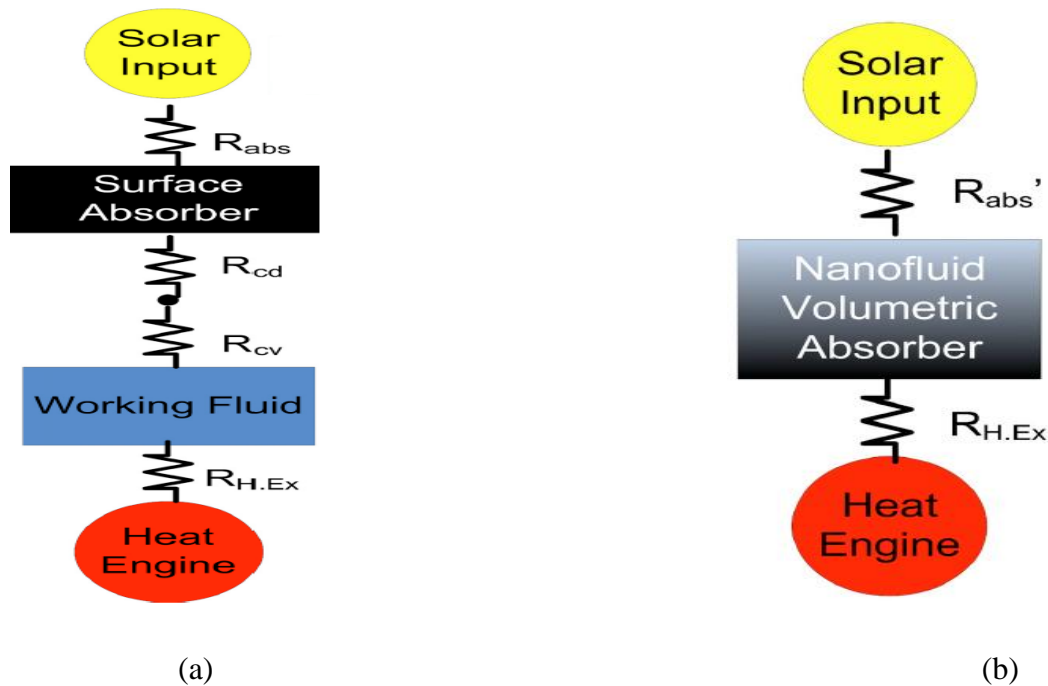


Fig 1.3 DASC(a:Conventional collector b: Direct Absorption solar collector)[5]

To enhance the efficiency of the solar collectors the system is made to directly absorb the solar energy within the fluid volume and thus so called Direct Absorption Solar Collector (DASC)[5]. The performance of collector not only depends on how effective the absorber is but also how effective is the heat transfer and thermal properties (e.g. Thermal Conductivity, Heat capacity) of the fluid. The absorption properties of the fluids generally used in solar collectors are very poor which in turn limits the efficiency of the solar collector and in this types of solar collectors all of the heat is to be absorbed by the working fluid so the heat absorption properties of the working fluid should be high. So, there is a need to use energy – efficient heat transfer fluids to get high efficiency. This need then results in the use of nanofluids in solar collectors.

### 1.3 Nanofluids[6]

Downscaling or miniaturization has been a recent major trend in modern science and technology. Engineers now fabricate microscale devices such as microchannel heat exchangers, and micropumps that are the size of dust specks. Further major advances would be obtained if the coolant flowing in the microchannels were to contain nanoscale particles to enhance heat transfer. When noble prize winner Richard Feynman presented the concept of

micromachines in 1959, miniaturization has been a major trend in modern science and technology. The concept and development of nanofluids is directly related to trends in miniaturization and nanotechnology. Just as downsizing is a fashion in the world of business, downscaling is a clear trend in the world of science and technology. One feature of these rapidly emerging technologies is that they are strongly interdisciplinary. A variety of micro-scale products are already available, or soon will be. Miniaturized sensors, actuators, motors, heat exchangers, pumps, heat pumps, valves, heat pipes, fuel cells, instruments, medical devices, robots, and airplanes are just a few of the almost endless variety of micro products in the market or poised to move from the laboratory to the marketplace. The electronics industry has applications in cooling advanced electronic packages; for the automotive industry, the weight difference between conventional and microchannel systems (such as in Air-conditioners) could lead to significant gains in fuel economy: in the HVAC industry). refrigeration and air conditioning equipment volumes could be reduced and this would save space in buildings; and in chemical and petroleum plants. plant size could be reduced through “process intensification.” After nanotechnology will come a technology for building up systems and structures from atoms and molecules via nanoparticles, nanotubes, and nanolayers. One can imagine that once scientists and engineers reach the atomic and molecular scale, they will be able to build systems and structures by using bottom-up methods, starting from atoms and molecules, rather than current top-down methods such as micromachining, lithography, and etching etc.

Nanofluids( Nanoparticle fluid suspension) is the term coined by choi(1995) to describe this new class of nanotechnology-based heat transfer fluids that exhibit thermal properties superior to those of their host fluids[7]. The goal of nano-fluids is to achieve the highest possible thermal properties at the smallest possible concentrations by uniform dispersion and stable suspension of nanoparticles in host fluids. Nano-fluids are having different properties as compared to the base fluid because in the nanoscale range ,the fundamental properties of nanomaterials such as nano-fluids depend strongly on particle size, shape and the surface/interface area. Earlier the heat transfer of the fluids is increased by the conventional methods of suspending micrometer or millimeter sized particles in the base fluid. The major problem with these fluids is the rapid settling of micrometer or millimeter sized particles and also these particles cannot be used in microchannels because they can clog micro channels. Choi in 1995 presented the remarkable possibility of doubling the convection heat transfer coefficients using nano-fluids instead of increasing pumping power. As nanofluids have improved thermal properties a study is carried out to investigate the performance of solar

collector using nanofluids. Nanofluids can replace conventional heat transfer fluids in solar collectors without increasing the pumping power of the system.

### **1.3.1 Preparation methods for nanoparticles[8]**

Preparation of nanoparticles can be classified into two broad categories : 1) Physical Processes 2) Chemical Processes.

Physical Processes include: 1)Inert Gas Condensation 2) Mechanical Grinding

Chemical Processes include:1) Chemical vapour deposition 2)chemical precipitation 3) Micro emulsions 4) Thermal Spray 5) Spray pyrolysis

### **1.3.2 Preparation methods for nanofluids**

Stable suspensions of nanoparticles in conventional heat transfer fluids are produced by two methods: 1)Two step method and 2)Single step method.

#### **1.3.2.1 Two step method**

Two-step method is the most widely used method for preparing nanofluids. Nanoparticles, nanofibers, nanotubes, or other nanomaterials used in this method are first produced as dry powders by chemical or physical methods. Then, the nanosized powder will be dispersed into a fluid in the second processing step with the help of intensive magnetic force agitation, ultrasonic agitation, high-shear mixing, homogenizing, and ball milling. Two-step method is the most economic method to produce nanofluids in large scale. Due to the difficulty in preparing stable nanofluids by two-step method, several advanced techniques are developed to produce nanofluids, including one-step method.

#### **1.3.2.2 Single step method**

The one-step process consists of simultaneously making and dispersing the Nanoparticles in the fluid. In this method, the processes of drying, storage, transportation, and dispersion of nanoparticles are avoided, so the agglomeration of nanoparticles is minimized, and the stability of fluids is increased. The one-step processes can prepare uniformly dispersed nanoparticles, and the particles can be stably suspended in the base fluid. One-step physical method cannot synthesize nanofluids in large scale, and the cost is also high, so the one-step chemical method is developing rapidly. However, there are some disadvantages for one-step

method. The most important one is that the residual reactants are left in the nanofluids due to incomplete reaction or stabilization. It is difficult to elucidate the nanoparticle effect without eliminating this impurity effect.

### LITERATURE REVIEW

As nanofluids have potential use in the field of energy transfer processes a detailed literature survey is presented on their properties and their application in solar energy. Firstly the literatures based on solar energy collectors are reviewed and the variations of efficiency to some parameters e.g. solar radiation, Mass Flow rate, Temperature difference etc is observed. Some papers and books are followed for the knowledge of Nanofluids and their thermal behaviour, how thermal property changes according to the volume fraction of nanoparticle in base fluid. Literature report also highlights the factors responsible for the improved properties of nanofluids and solar collectors.

Literature of Nanofluids application in solar collectors is studied profoundly.

#### **Otanicar P T *et al.*[9]**

This paper states that in direct absorption solar collectors, the efficiency is limited by the absorption properties of the working fluid which is very poor for conventional fluids used in solar collectors. It has been shown here that mixing nano-particles in a base fluid has dramatic effect on the thermophysical properties such as thermal conductivity[]. Nano particles also increases the radiative properties of liquids, leading to an increase in the efficiency of direct absorption solar collectors. The reason for using direct absorption solar collector is that in case of using a absorber surface to collect solar radiations, which after collection transfers the heat to the working fluid, the efficiency is not only limited by the how effectively the absorber surface captures solar energy but also how effectively the heat is transferred to the working fluid whereas in case of direct absorption solar collector the solar radiation directly strikes on working fluid . One of unique benefits of using nanofluids is that when nanofluids are used the absorption spectrum is typically broadened. This broadening allows the nanofluids to absorb a larger portion of the spectrum. Besides all the benefits to the radiative and optical properties, nanofluids also provide improvements in operating efficiency of direct absorption solar collector.

In this paper two parameters of nanofluids are varied: volume fraction of the nanoparticle in the base fluid and varying particle size. Three different groups of nanofluids, with water as the base fluid are considered: Graphite sphere based ,carbon nanotubes ,and silver sphere based. These fluids are tested by varying volume fraction and particle size.

The test apparatus used in this experiment has the following dimensions and characteristics: Collector area  $3 \times 5 \text{ cm}^2$  area with a channel depth of  $150 \mu\text{m}$ . The microchannel geometry was selected to minimize the use of nanofluids. The collector glazing is a low reflectance glass of thickness  $3.3 \text{ mm}$  for all experiments. The collector back surface was coated with a reflective aluminium tape for all experiments with nanofluids and one experiment with water. Three T-type thermocouples were mounted to measure the inlet and outlet temperatures of the fluid. The whole of the system is insulated with styrofoam block to limit heat loss from the back and sides of the collector. The flow rate was controlled via a syringe pump and was set to  $42 \text{ ml/h}$ .

Results:

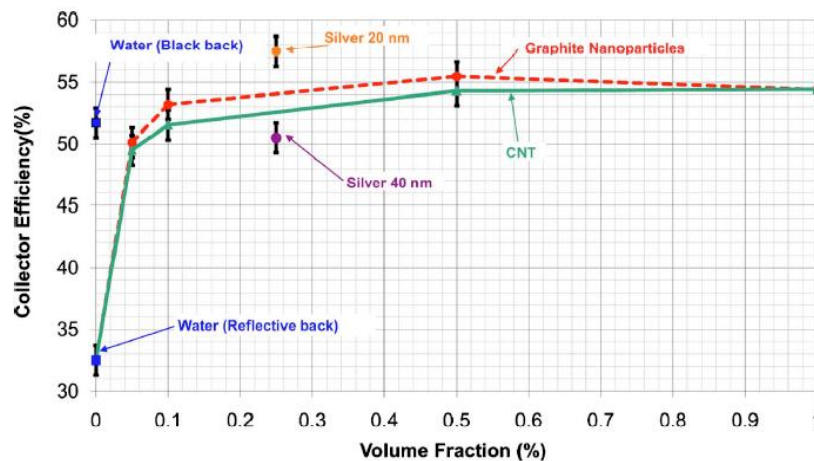


**Fig 2.1(Variation of collector efficiency with volume fraction)**

Efficiency is the ratio of usable thermal energy to the incident solar energy. In Fig the variation of efficiency and volume fraction of nanoparticle in base fluid is shown. The small increase in volume fraction of nanoparticles results in a rapid efficiency enhancement. By using  $20 \text{ nm}$  silver nanoparticles an increase in efficiency of  $5\%$  can be achieved

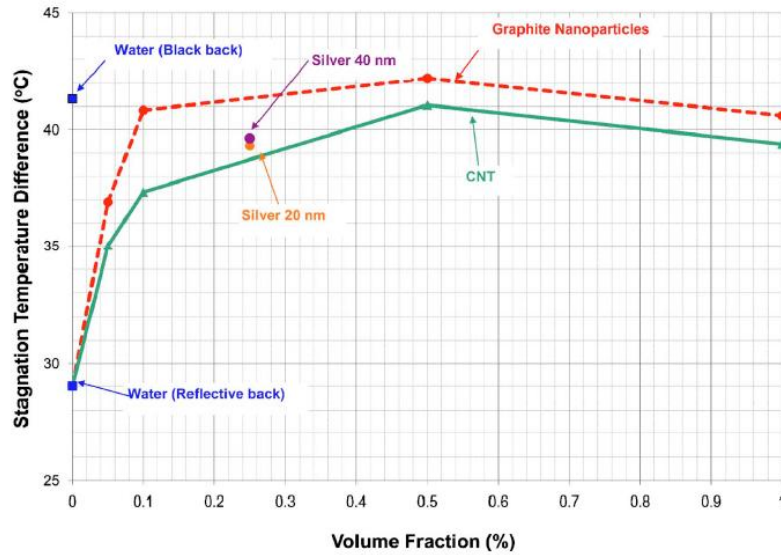


**Fig 2.2(Variation of stagnation temperature difference with volume fraction)**

The plot between Temperature difference and volume fraction shows the same pattern. Again a rapid increases in the temperature difference as volume fraction of nanoparticles is increased

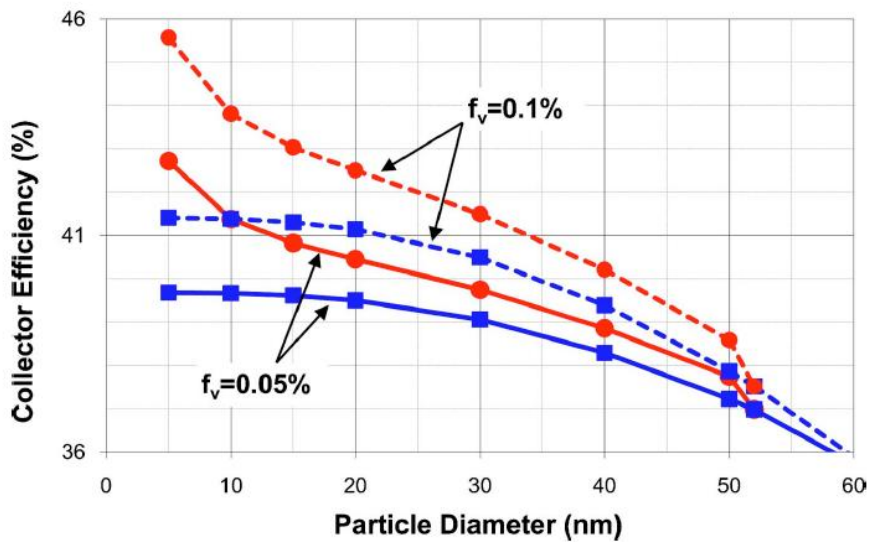


**Fig.2.3(Collector Efficiency as a function of silver nanoparticle diameter and volume fraction)**

The above plot shows that the reduced size nanoparticle further leads to an even higher efficiency. In the plot squares shows the bulk properties and circles represents size dependent properties

### **Tyagi H *et al.*[10]**

This paper theoretically investigates the feasibility of using a flat plate collector with nanofluids and compares its performance with that of a conventional flat plate collector. Here nanofluid a mixture of water and aluminium nanoparticles is used as the absorbing medium. A two-dimensional heat transfer analysis was developed in which direct sunlight was incident on a thin flowing film of nanofluid. The model accounted for the incident sunlight and included the effects of absorption and scattering by the working medium. It was observed that the efficiency of a nanofluid DAC is a function of various geometrical parameters and operating conditions.

In this paper following results were found:

- (a) The collector efficiency was found to increase with particle volume fraction, glass cover transmissivity and the collector height.
- (b) The particle size and length of collector did not significantly influence the collector efficiency.
- (c) The results showed about 10% higher absolute efficiencies for the nanofluid-based direct absorption solar collector in comparison with conventional flat-plate type collectors that use pure water under similar operating conditions.

### **Taylor R A *et al.*[5]**

This paper is the analysis of how nanofluid based concentrating solar collector would compare to a conventional one. Efficiency improvement on the order of 5 – 10% can be achieved in a nanofluid receiver. This paper also depicts that as solar power plant move to larger scale nanofluids show even more potential. In this research work a new receiver is designed. The nanofluid used for this work consist of Therminol VP – 1 heat transfer oil as base fluid and graphite nanoparticles are dispersed in the base fluid. The volume fraction is used as 0.125% and 0.25%. As concentrating solar collector has a greater concentration ratio, so their efficiency is also higher.

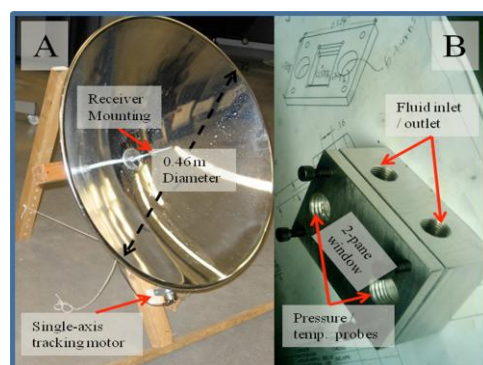


**Fig 2.4(A-reflective Dish,B-machined aluminium part with inlet and outlet ports)**

In Fig part B is the receiver the gap between the plates is 1mm, and dimensions are as follows:

Area of receiver = 2cm x 2cm

Operating Temperature = 270°C

Mass flow rate =  $1 \times 10^{-4}$  kg/s

Dish Concentration ratio = 400

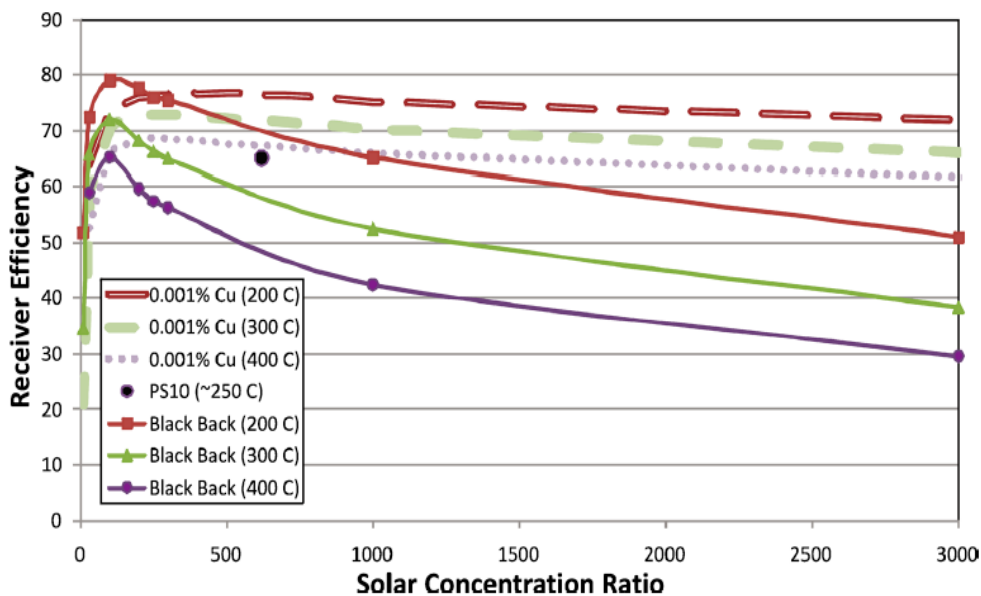


**Fig2.5(Variation of receiver efficiency with solar concentration ratio)**

The Fig 2.5 shows model results for the pure base fluid i.e., nearly non absorbing with a selective surface “black backing” under similar receiver operating conditions. The results in Fig illustrate that a nanofluid collector may operate more efficiently than a conventional surface solar collector under optimum conditions, up to 10% higher for solar concentration ratios in the range of 100–1000. As shown in the figure, the nanofluid and its operating conditions must be chosen carefully or the system may end up operating less efficiently.

This paper also describes the economic implications for the application of nanofluid in high flux solar collector. Nanofluids are not expected to be suitable for dish or trough solar power system one big reason for that is the high cost and economic factors

### **Han z.[12]**

Heat transfer fluids have inherently low thermal conductivity that greatly limits the heat exchange efficiency. Liquid dispersions of nanoparticles, which have been termed “nanofluids”, exhibit substantially higher thermal conductivities than those of the corresponding base fluids. In this paper the thermal transport properties of nanofluids including thermal conductivity, viscosity, heat capacity and heat transfer coefficient in convective environment were characterized and modelled. Obvious thermal conductivity increases have been observed in these nanofluids. Since the heat capacity of heat transfer fluids is another important thermal transport property upto 126% and 20% increases in the effective heat capacity were experimentally found in water nanofluids. The results show that nanofluids possess improved thermal transport properties and it has been experimentally proved that nanofluids have potential as next generation advanced heat transfer fluids.

### **Trisaksri v *et al.*[13]**

This paper is the review of recent research developments on the heat transfer characteristics. The transient hot wire method , temperature oscillation and steady-state parallel plate method has been employed to measure the thermal conductivity of nanofluids.

The experimental results showed that the thermal conductivity of all nanofluids were higher than those of their base fluids. The thermal conductivity of the nanofluids increased with increasing volume fraction of nanoparticles. For a specific volume fraction, the increase of thermal conductivity was different for each base fluid. The thermal conductivity enhancement of nanofluids depends on the particle volume fraction, size and shape of nanoparticles, type of base fluids and nanofluids .

Wang *et al*<sup>10</sup>., used the steady-state parallel-plate technique to measure the thermal conductivity of nanofluids containing Al<sub>2</sub>O<sub>3</sub> and CuO nanoparticles. The particles were dispersed in water, ethylene glycol, vacuum pump oil and engine oil. Experimental data showed that the thermal conductivity of all nanofluids were higher than those of their base fluids. The thermal conductivity of the nanofluids increased with increasing volume fraction of the nanoparticles. For a specific volume fraction, the increase of thermal conductivity was different for each base fluid. The natural convection of fluid small-particles suspensions has

been used in many applications in the chemical industry, food industry and also in solar collectors<sup>12</sup>. The thermal conductivity enhancement of nanofluids depends on the particle volume fraction, size and shape of nanoparticles, type of base fluid and nanoparticles, pH value of nanofluids and type of particle coating. The natural convective heat transfer of nanofluids is different from that of the common suspensions in that the particles concentration gradient is absent<sup>11</sup>.

#### **Yousefi T *et al.*[14]**

In this paper efficiency variation of flat plate solar collector for Al<sub>2</sub>O<sub>3</sub>-H<sub>2</sub>O based nanofluids is presented for various mass flow rates and also the effect of addition of surfactants on the efficiency of collectors is studied. The volume fraction of nanoparticles was 0.2% and 0.4% and the particles dimension was 15 nm. Experiments were performed with and without Triton X-100 as surfactant. The mass flow rate of nanofluid varied from 1 to 3 Lit/min. In this paper ASHRAE Standards were followed. All the chemicals used in the experiments were of reagent grade. Commercial spherical-shape Al<sub>2</sub>O<sub>3</sub> powders (M K impex Canada) with 99.5% of purify and an average diameter of 15 nm was used. Triton X-100 from Merck was used as natural surfactant for dispersion of Al<sub>2</sub>O<sub>3</sub>. The double distilled water was used throughout the studies as a base fluid. In order to minimize Al<sub>2</sub>O<sub>3</sub> aggregation and improve dispersion behavior, two impressive methods were performed in this investigation. (1) Using Triton X-100 as the dispersant and (2) using ultrasonic vibration (with UP-400S ultrasonic model).

For calculating the efficiency of the collector ASHRAE Standards have been followed.

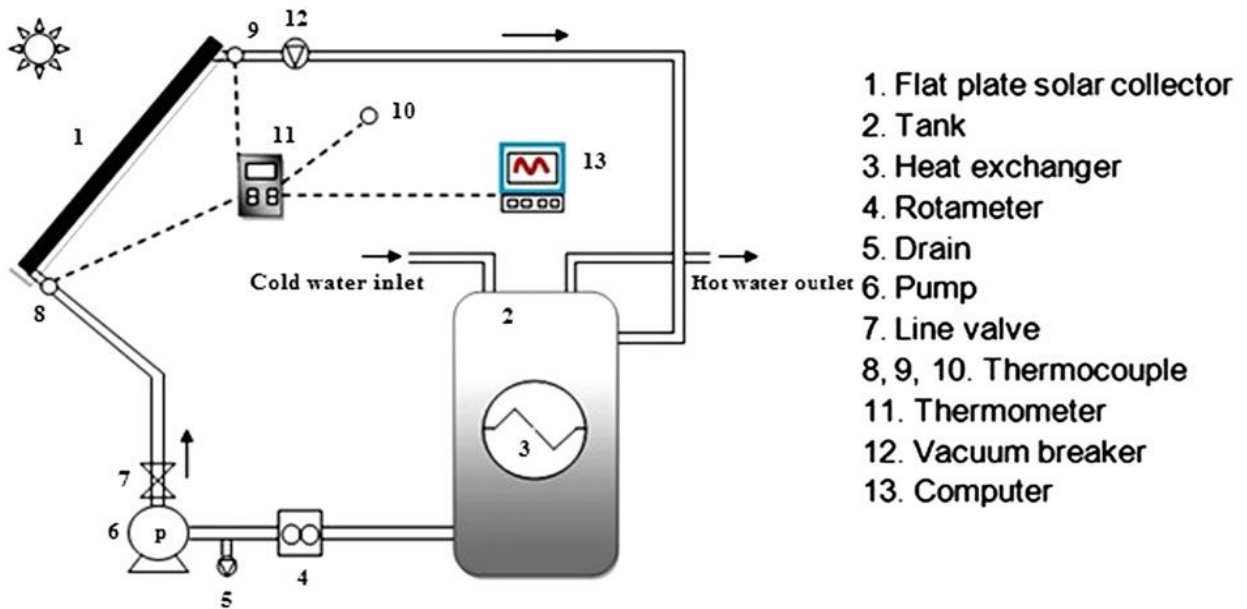


**Fig. 2.6(Schematic Diagram of the collector)**

The tests have performed around solar noon at time 10 to 15. The experimental results are presented in the form of graphs and equations that describe the collector efficiency against a reduced temperature parameter,  $(T_i - T_a)/G_T$ .

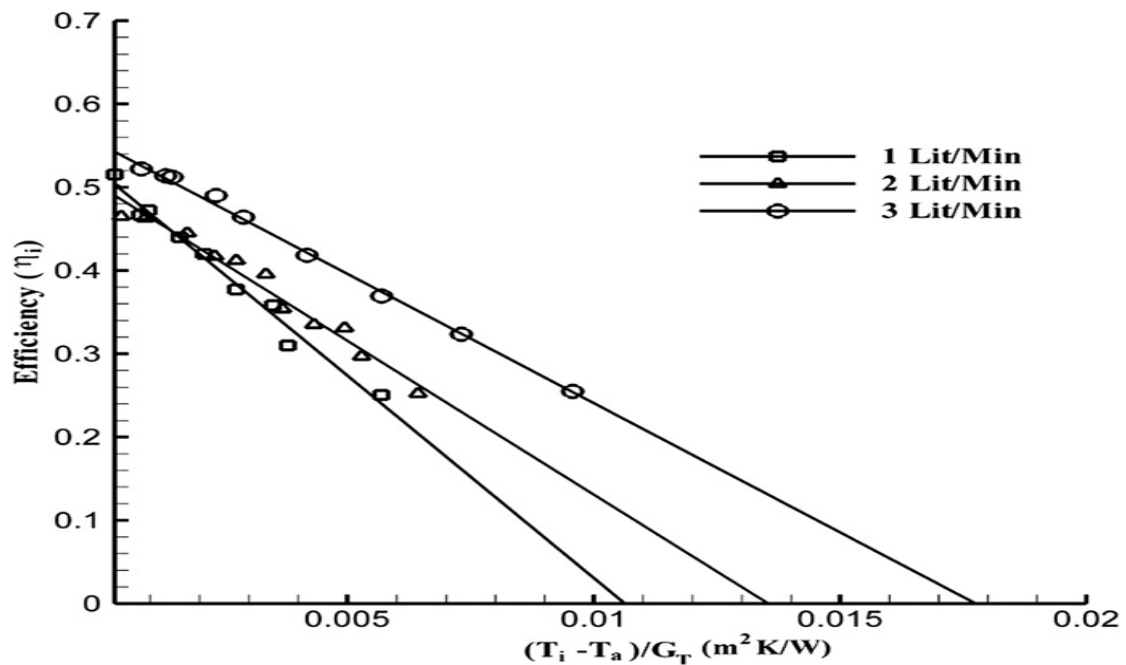


**Fig2.7(variation of collector efficiency at different mass flow rates)**

The solar collector was tested for various mass flow rates of 1, 2, and 3 Lit/min. Each test was performed in several days and the best experimental data has been chosen. From the plot this can be concluded that the for higher mass flow rate the efficiency of the collector is high.

As the mass flow rate is reduced the collector efficiency also decreases. The experimental data are fitted with linear equations to provide the characteristic parameters of the flat-plate solar collector in order to compare the effect of various mass flow rates.

Al<sub>2</sub>O<sub>3</sub> nanofluid without surfactant as working fluid:

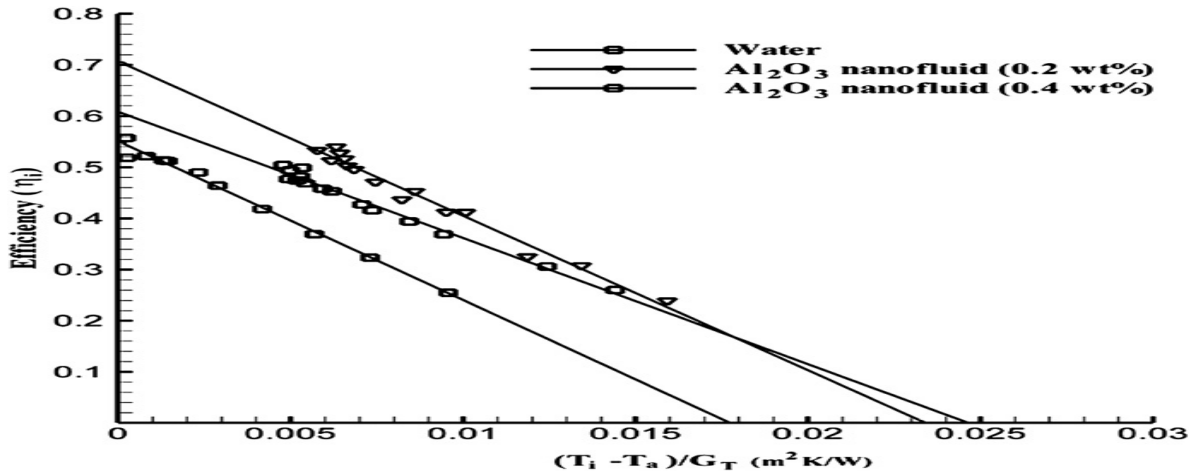


**Fig 2.8 ( Effect of nanofluids on the efficiency of the collector)**

By comparing these two plots this can be concluded that efficiency of the collector increases by addition of the nanoparticles to the conventional fluid.

The effect of using the Al<sub>2</sub>O<sub>3</sub> nanofluid as absorbing medium in a flat-plate solar water heater is investigated. The results show that using the 0.2 wt% Al<sub>2</sub>O<sub>3</sub> nanofluid increases the efficiency of solar collector in comparison with water as working fluid by 28.3%.

**Timofeeva V E *et al.*[15]**

In this paper an overview of systematic studies that address the complexity of nanofluid system and advance the understanding of nanoscale contributions to viscosity, thermal conductivity and cooling efficiency of nanofluids is presented. A nanoparticle suspension is considered as a three phase system including the solid phase(Nanoparticles), the liquid phase (fluid media),and interfacial phase which contributes significantly to the system properties because of its very high surface to volume ratio in nanofluids. The initial promise of nanofluids as advanced heat transfer fluids was based on the increased thermal conductivity of nanoparticle suspensions. Low thermal conductivity of conventional fluids improves when the solid particles are added. Great varieties of nanoparticles are commercially available and can be used for preparation of nanofluids. Nanoparticle material, concentration, size, and shape all contribute to the nanofluid properties. The size of nanoparticles defines the surface-to-volume ratio and for the same volume concentrations suspension of smaller particles will

have a higher area of the solid/ liquid interface. Therefore, the contribution of interfacial effects will be stronger in such a suspension. The size of nanoparticles also affects the viscosity of nanofluids. In general, the viscosity increases as the volume concentration of particles increases. Studies of suspensions with the same volume concentration and material of nanoparticles but different sizes showed that the viscosity of suspension increases as the particle size decreases. The relative importance of engineering parameters resulted from such analysis suggests the potential nanofluid design options. Importantly, the criteria are not weighted to allow a quick selection process. The nanoparticle concentration, base fluid, and particle size appear to be the most influential parameters for improving the heat transfer efficiency of nanofluid.

**Wang.X.Q.*et al.*[23]**

In this paper a study of fluid flow and heat transfer properties of nanofluids in forced and free convection systems are done. The convective heat transfer can be enhanced by changing flow geometry, boundary conditions or by enhancing thermal conductivity of the fluid. They have measured the relative viscosity for  $\text{Al}_2\text{O}_3\text{-H}_2\text{O}$  and  $\text{Al}_2\text{O}_3\text{-ethylene glycol}$  nanofluids, the results observed showed the similar trend of increase of relative viscosity. The addition of nanoparticles showed the increase in the heat transfer. Also, it has been found that for nanofluids the value of convective heat transfer coefficient is higher than conventional heat transfer fluid.

### OBJECTIVES

The efficiency of solar collector mainly depends on the fluid that is absorbing the heat. So it has been found that the thermal properties (Specific heat, Heat capacity, viscosity, density etc.) of the fluid that is passing through the collector plays an important role to make the system more effective. By reviewing the past research it has been concluded that conventional fluids can absorb heat up to a certain limit which, in turn, limits the efficiency of solar collector, where as recently developed new class of fluids called “Nanofluids” possesses very good thermal properties. So these nanofluids can be used in solar collectors in order to improve its performance. So, In this thesis we are going to evaluate the performance of flat plate solar collectors using nanofluids.

The main objectives of this Experimental work are as follows:

1. To investigate the variation of collector efficiency throughout the day (hourly) using nanofluid (water based  $\text{Al}_2\text{O}_3$ ).
2. To investigate the variation of collector efficiency throughout the day using water.
3. To investigate the variation of collector efficiency with varying volume fraction.
4. To examine the temperature variation throughout the day (hourly).
5. Comparison of performance of solar collector for nanofluid and water.

### METHODOLOGY

In this chapter , discussion about experimental setup, dimensions, standards followed and instruments used in performing the experiments are discussed.

In performing the experiments ASHRAE Standards are followed. The list of ASHRAE Standards are as follows :

#### 4.1 ASHRAE Standards 93 – 77[16,17]

The Conduct of the efficiency Tests as specified in ASHRAE Standards 93 – 77 are as follows:

1. For the measurement of solar radiation in the plane of the collector, a pyranometer as classified by the World Meteorological Organization should be used.
2. Data should be taken during the middle of the day, preferably when the solar incident angle is less than  $30^\circ$ .
3. A series of tests should be conducted, each of which determines the average efficiency of a 5 – min period.
4. In computing efficiency, the gross frontal area is used instead of aperture area.
5. The efficiency curve is drawn by plotting efficiency as a function of the difference between the inlet fluid temperature and the ambient temperature divided by the incident solar radiation.
6. The collector is required to undergo a preconditioning test prior to the start of thermal tests. The collector must be exposed for three consecutive days with no fluid passing through it and with the mean incident solar radiation measured in the plane of the collector aperture exceeding  $17,000 \text{ kJ/m}^2$  days.
7. Before the efficiency test, the time constant is determined. The time constant test determines the transient thermal properties of the collector.
8. The entire group of test may be made in doors using a solar simulator if desired

9. After the efficiency tests are completed, a series of tests is conducted to determine the collector's incident angle modifier. The collector's incident angle modifier test consists of a series of efficiency determinations for a range of incident angles, with the inlet fluid temperature of the collector equal to the ambient temperature.
10. The inlet fluid temperature to the collector must be adjusted and controlled to a desired value.
11. On any given day, data is recorded under steady state conditions for fixed values of mass flow rate and inlet temperature.

## 4.2 Experimental Set – Up

The model of test apparatus is shown in Fig.4.1. The micro channel geometry is used in order to minimize the amount of nanofluids needed for the each test. In the experiment  $\text{Al}_2\text{O}_3\text{-H}_2\text{O}$  based nanofluids with different concentrations are used. An Infusion Set is used to maintain the constant mass flow rate of the nanofluid through the set-up.

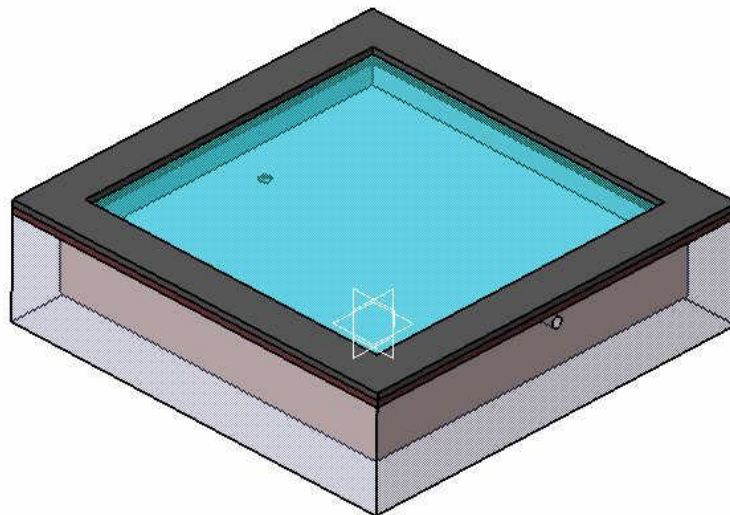


**Fig. 4.1 (3D Model of the experimental set-up)**

The collector glazing is low reflectance glass which acts as transparent to the incoming short wavelength solar radiations but becomes opaque for high wavelength radiations emitted by the Absorber plate. In this collector we are using Direct Absorption system in which the solar radiations are directly allowed to strike the working fluid. so, the conduction and convection losses are eliminated in this collector.

The instantaneous efficiency of the solar collector<sup>18</sup> can be calculated using:

$$\eta = m C_{\text{eff}}(T_2 - T_1) / G_T A$$

$$m = \rho_{\text{eff}} \times A \times v$$

$$\rho_{\text{eff}} = (1 - \phi_p) \rho_f + \phi_p \rho_p$$

$$\phi_p = V_p / (V_p + V_f)$$

$$C_{\text{eff}} = \{ (1 - \phi_p) \rho_f c_f + \phi_p \rho_p c_p \} / \rho_{\text{eff}}$$

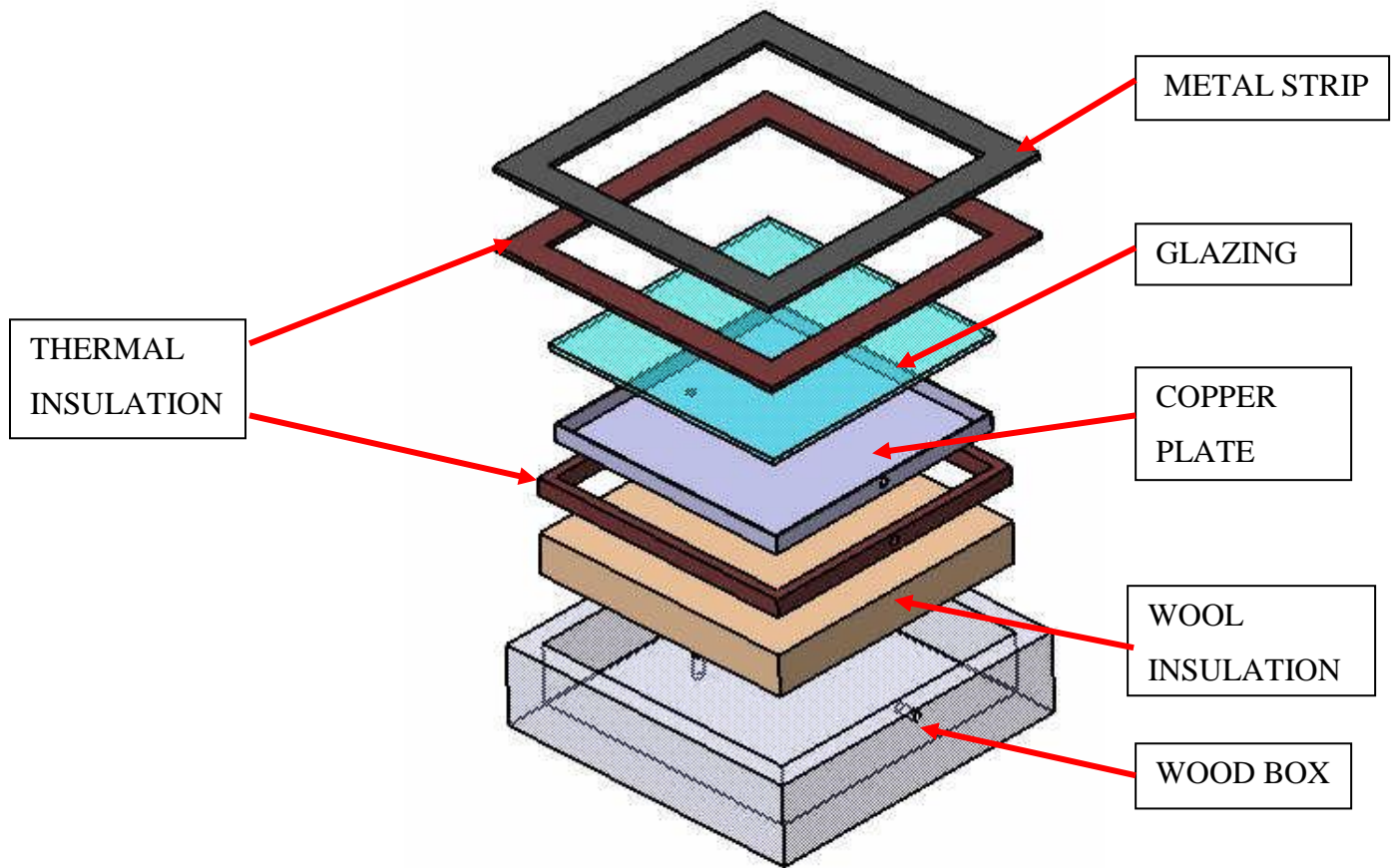


**Fig. 4.2:(Exploded view of Apparatus)**

In order to minimize the losses proper insulation is provided in the collector. For insulation thermocol and glass wool are used. Thermocol insulation is given between the gap of copper plate and wood box. Wool insulation is given at the bottom of the copper plate to prevent the heat losses from the bottom.

The dimensions of the apparatus are shown in Fig.4.3

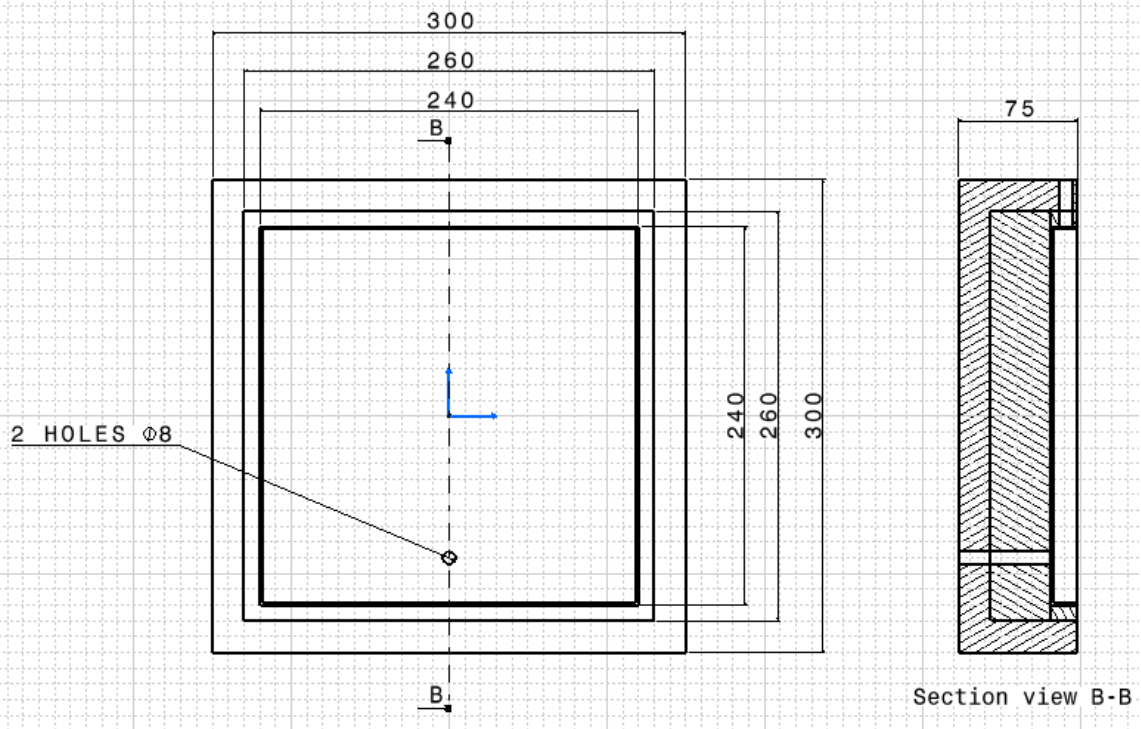


**Fig. 4.3:(Dimensions of the collector)**



**Fig 4.4:Actual view of Flat plate direct absorption solar collector**

### 4.3 Preparation of Nanofluids

a) Purchased Sample of Nanoparticles:

Al<sub>2</sub>O<sub>3</sub> Nanoparticles were purchased from Reinste Nanoventures Pvt. Ltd. New Delhi.

Specifications of Nanoparticles:

Particle shape: Spherical

Average Particle Size: 40 nm

Particle size full Range: 5-150nm

Specific Surface: >10m<sup>2</sup>/g

Purity: >99.8%

#### 1) Structural Characterization

Structural Characterization of nanoparticles can be done by using techniques such as BET, XRD, SEM, TEM, and HRTEM. As this research work is more concerned about the application of nanofluids so XRD and TEM analysis is done for the authentication of nanoparticles.

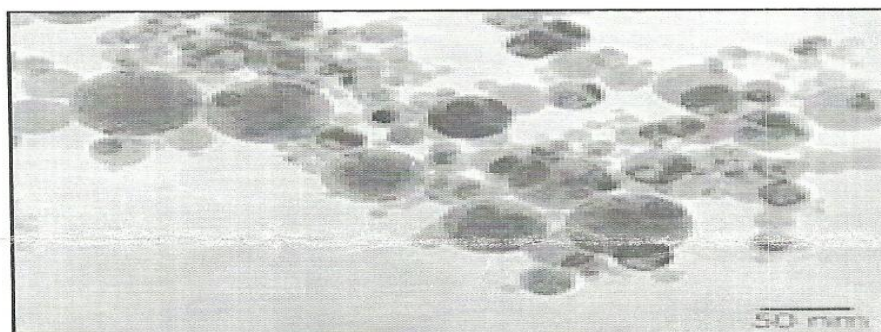
#### TEM of Purchased Sample

Al<sub>2</sub>O<sub>3</sub> - Nanopowder, alpha

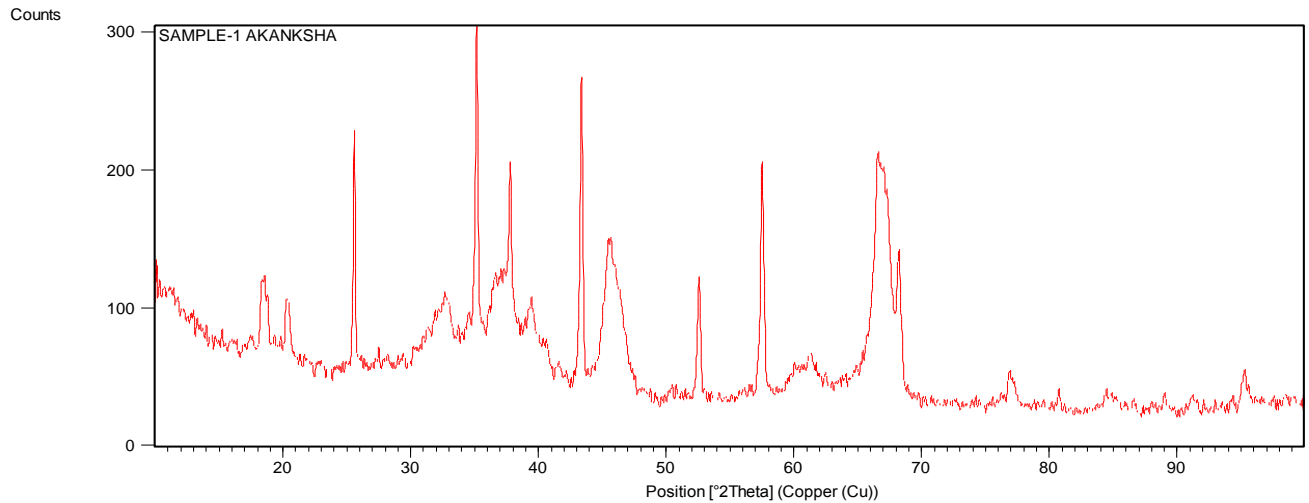
Catalog No: RN-PL-A-ALO-10g

Particle shape: spherical  
Average particle size: ca. 40 nm  
Specific surface: > 10 m<sup>2</sup>/g  
Purity: > 99.8 %  
X-Ray analysis: α-Al<sub>2</sub>O<sub>3</sub>

TEM Image



## XRD of purchased sample



## 2) Sonication of Nanoparticles[19]

To prepare the  $\text{Al}_2\text{O}_3$  nanofluid, there is a need to determine the weight of  $\text{Al}_2\text{O}_3$  for different concentration. The weight of  $\text{Al}_2\text{O}_3$  can be evaluated by using the standard expression.

$$X^{20} = V_P / V_{\text{eff}}$$

Where,  $V_P = W_P / \rho_P$

$$V_{\text{eff}} = V_P + V_f, V_f = W_f / \rho_f$$

Quantity of Base fluid (Water),  $V_f = 500\text{ml}$

Density of  $\text{Al}_2\text{O}_3$  particles,  $\rho_P = 3.9 \text{ gm/cm}^3$

Density of water,  $\rho_f = 1000 \text{ kg/m}^3$

Table 4.1: Shows the weight of  $\text{Al}_2\text{O}_3$  particles to prepare the nanofluid of different concentration.

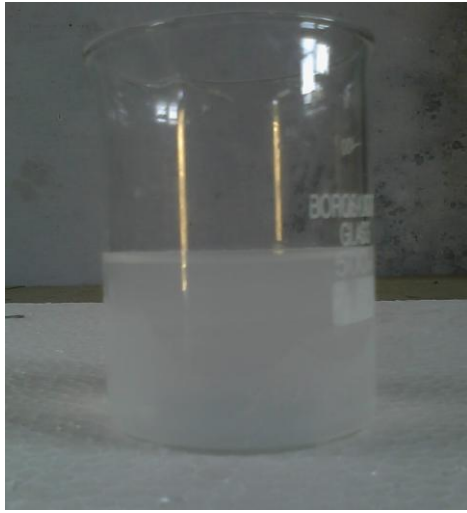
|       |        |         |         |
|-------|--------|---------|---------|
| X     | 0.005  | 0.05    | 0.1     |
| $W_p$ | .09912 | 0.99174 | 1.98448 |

After calculating the desired weight of the nanoparticles for a particular volume fraction the required amount of distilled water is poured into it. After pouring distilled water to it then sonication of the fluid takes place for 6 hours. After sonication the uniformly dispersed nanofluids are ready to flow.

The sonicator used for the sonication of the nanofluids is oscar ultra sonicator which was probe type .



**Fig 4.5: Oscar Ultra Sonicator (Probe Type)**



(a)



(b)

**Fig. 4.6 (a) ( $\text{Al}_2\text{O}_3\text{-H}_2\text{O}$ ) Nanofluid (with 0.005% volume Concentration)**

**(b) ( $\text{Al}_2\text{O}_3\text{-H}_2\text{O}$ ) Nanofluid (with 0.05% volume Concentration)**

#### 4.4 Instruments

Various instruments needed for the experiment as follows

- 1) Pyranometer
- 2) Digital Thermometer
- 3) Infusion Set

## Pyranometer[21]

A pyranometer is an instrument that measures the total amount of sunlight reaching a horizontal plane on earth's surface. This quantity is called "Insolation". It is typically measured in metric units of watts per square meter( $W/m^2$ ). The term pyranometer is originated from greek word "pyr" meaning "fire" and "ano" meaning "above sky" which means fire coming from the sky. It measures both beam as well as diffused solar radiations.

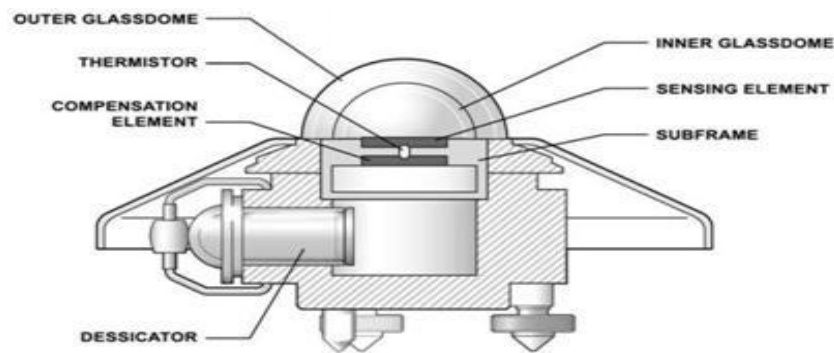


Fig. 4.7

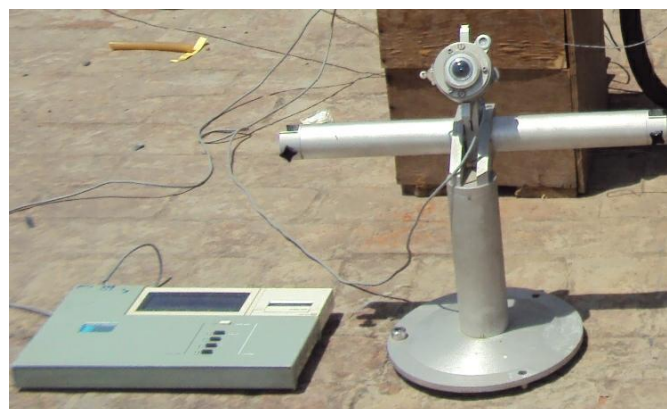


Fig. 4.8 (Kipp & Zonen Pyranometer)

A solar pyranometer[22] works by measuring the number of photons, small units of light, that impact either a chemical or physical device within the instrument over time. Physical types of pyranometers include bolometers, thermopiles and photodiodes. Bolometers use a thin layer of metal attached to a heat sink which maintains a constant temperature, allowing the device to recognize solar radiation levels. Thermopiles convert heat into electricity through coupled devices in a series, measuring voltage output to determine radiation. Photodiodes use a similar technique to convert light into current or voltage, allowing measurement. The level of possible measurement in a pyranometer varies depending on the position of the Sun itself. Ideal conditions are supplied by the Sun being directly overhead, however, certain measurements can be made from different angles, as long as the radiation impact is identified. The thermopile sensor generates a voltage output signal that is proportional to the solar radiation. The Pyranometer does not require any power

The pyranometer used for the measurement of the solar radiation is shown in Fig. 4.6.

Company Name: KIPP & ZONEN

Model No. : CMP – 11

Operating Temperature Range:  $-40^{\circ}\text{C}$  to  $+80^{\circ}\text{C}$

Maximum Solar Irradiance Measurement:  $4000\text{ W/m}^2$

Field of view:  $180^{\circ}$

### **Infusion Set**

The purpose of infusion set is to deliver glucose or blood under the skin. This instrument is used in medical treatments. Very low mass flow rate can also be achieved using this device. The fluid flow is under gravity effect.

According to the specification 20 drops of fluid makes 1ml ( $\pm 0.1\text{ml}$ ).

So, For 60 ml/hr

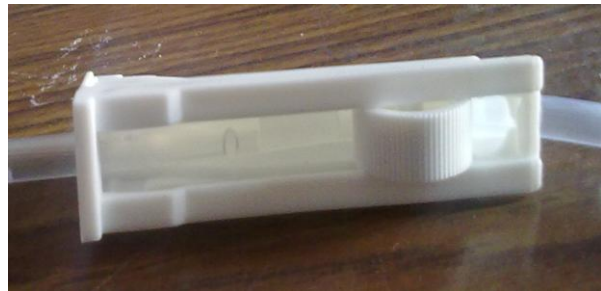
No. of drops = 20 / min.

For 80 ml/hr

No. of drops = 27 / min.

For 100 ml/hr

No. of drops = 33 / min.



(a) Infusion set attached with storage bottle

(b) Flow control mechanism

**Fig 4.9**

### **Digital Thermometer**

Manufacturer: Mextech

Temperature Range:  $-50^{\circ}\text{C}$  to  $+200^{\circ}\text{C}$

Temperature Resolution:  $0.1^{\circ}\text{C}$

Temperature Accuracy:  $\pm 1^{\circ}\text{C}$  upto the range of  $150^{\circ}\text{C}$

## **RESULTS AND DISCUSSIONS**

In this chapter the Results which were obtained by performing various experiments on solar collector are presented. The results are shown in the form of graphs.

First of all the graphs are plotted with water and then with  $Al_2O_3$  with different concentrations.

### **5.1 Solar Collector Instantaneous Efficiency Calculations**

The instantaneous efficiency of the solar collector can be calculated as follows

$$\eta = m C_{\text{eff}}(T_2 - T_1) / G_T A C_r \quad (1)$$

$$m = \rho_{\text{eff}} \times A \times v \quad (2)$$

$$\rho_{\text{eff}} = (1 - \phi_p) \rho_f + \phi_p \rho_p \quad (3)$$

$$\phi_p = V_p / (V_p + V_f) \quad (4)$$

$$C_{\text{eff}} = \{ (1 - \phi_p) \rho_f c_f + \phi_p \rho_p c_p \} / \rho_{\text{eff}} \quad (5)$$

Where

$\eta$  = Instantaneous Efficiency

$m$  = Mass flow rate of the working fluid.

$C_{\text{eff}}$  = Effective specific heat of the Nanofluids.

$T_2$  = Outlet Temperature of the working fluid.

$T_1$  = Inlet Temperature of the working fluid.

$G_T$  = global solar irradiation

$A$  = Area of the Absorber Plate

$\rho_{\text{eff}}$ = Density of the Nanofluids

$\Phi_p$ = Volume fraction of Nanoparticle

$\rho_p$ = Density of nanoparticles

$V_p$ = Volume of the Nanoparticles

$V_f$ = Volume of the base fluid

**Table 5.1: Global solar irradiation Readings using Pyranometer ( $\text{W}/\text{m}^2$ )**

| <b>Time</b>    | <b>5/5/12</b> | <b>6/5/12</b> | <b>7/5/12</b> | <b>27/5/12</b> | <b>28/5/12</b> | <b>29/5/12</b> | <b>2/6/12</b> | <b>4/6/12</b> | <b>7/6/12</b> |
|----------------|---------------|---------------|---------------|----------------|----------------|----------------|---------------|---------------|---------------|
| <b>10:00AM</b> | 590           | 580           | 600           | 630            | 565            | 590            | 588           | 590           | 585           |
| <b>11:00AM</b> | 685           | 690           | 725           | 745            | 670            | 695            | 693           | 694           | 724           |
| <b>12:00PM</b> | 805           | 810           | 835           | 835            | 790            | 816            | 810           | 805           | 820           |
| <b>01:00PM</b> | 965           | 965           | 980           | 967            | 935            | 956            | 935           | 945           | 960           |
| <b>02:00PM</b> | 910           | 905           | 915           | 845            | 862            | 820            | 824           | 856           | 856           |
| <b>03:00PM</b> | 803           | 805           | 820           | 790            | 782            | 759            | 795           | 775           | 765           |

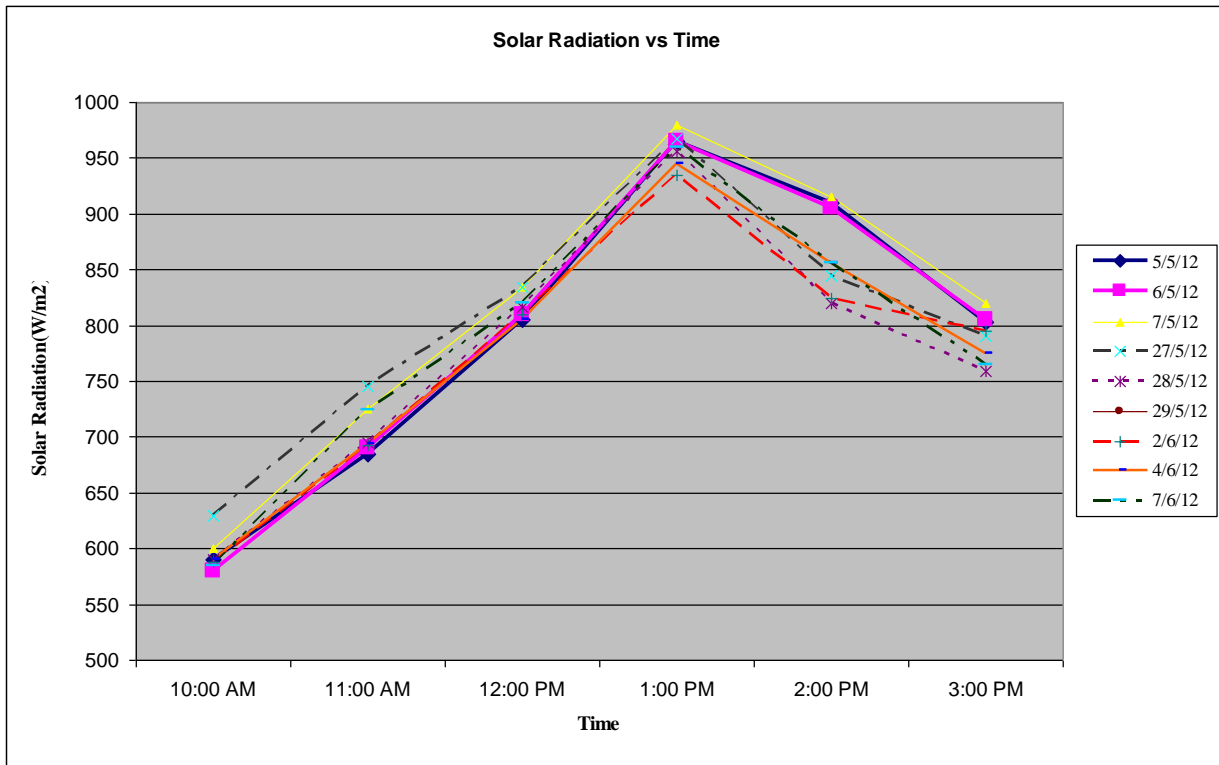


**Fig 5.1: Variation of global solar irradiance w.r.t time at different days**

Area of the Solar collector= 0.0576 m<sup>2</sup>

Total radiations intercepted by the solar collector =  $A \times G_T$  (W/m<sup>2</sup>)

According to ASHRAE Standards :

- a) Inlet temperature of the working fluid is assumed to be constant for all the experiments i.e 29<sup>0</sup>C.
- b) The Experiments are performed in the Solar noon i.e from 10 am to 3 pm.

**Table 5.2: Total Solar Radiation Incident on the solar collector**

| Time    | 5/5/12 | 6/5/12 | 7/5/12 | 27/5/12 | 28/5/12 | 29/5/12 | 2/6/12  | 4/6/12  | 7/6/12 |
|---------|--------|--------|--------|---------|---------|---------|---------|---------|--------|
| 10:00AM | 33.984 | 33.408 | 34.56  | 36.288  | 32.544  | 33.984  | 33.868  | 33.984  | 33.696 |
| 11:00AM | 39.456 | 39.744 | 41.76  | 42.912  | 38.592  | 40.032  | 39.9168 | 39.9744 | 41.702 |
| 12:00PM | 46.368 | 46.656 | 48.096 | 48.096  | 45.504  | 47.0016 | 46.656  | 46.368  | 47.232 |

|                |         |        |        |        |         |         |         |         |        |
|----------------|---------|--------|--------|--------|---------|---------|---------|---------|--------|
| <b>01:00PM</b> | 55.584  | 55.584 | 56.16  | 57.312 | 53.856  | 55.0656 | 53.856  | 54.432  | 55.296 |
| <b>02:00PM</b> | 52.416  | 52.128 | 52.704 | 48.672 | 49.6512 | 47.232  | 47.4624 | 49.3056 | 49.305 |
| <b>03:00PM</b> | 46.2528 | 46.368 | 47.232 | 45.504 | 45.0432 | 43.7184 | 45.792  | 44.64   | 44.064 |

**5.1.1. Performance evaluation of the collector using water as the working fluid**

For water,

Density  $\rho = 1000 \text{Kg/m}^3$

Specific Heat  $C_p = 4.187 \text{Kj/Kgk}$

Mass Flow Rate  $m = \rho \times V$

**Table 5.3: Mass Flow Rate**

| <b>Vol. flow Rate(ml/hr)</b> | <b>Mass flow Rate(Kg/sec)</b> |
|------------------------------|-------------------------------|
| 60                           | $1.66 \times 10^{-5}$         |
| 80                           | $2.22 \times 10^{-5}$         |
| 100                          | $2.77 \times 10^{-5}$         |

**Table 5.4: Temperature Readings for Water**

| <b>Time</b>    | <b>Temperature inlet(°C)</b> | <b>Temperature outlet(°C)</b> |                  |                   | <b>Temperature Difference(°C)</b> |                  |                   |
|----------------|------------------------------|-------------------------------|------------------|-------------------|-----------------------------------|------------------|-------------------|
|                |                              | <b>60(ml/hr)</b>              | <b>80(ml/hr)</b> | <b>100(ml/hr)</b> | <b>60(ml/hr)</b>                  | <b>80(ml/hr)</b> | <b>100(ml/hr)</b> |
| <b>10:00AM</b> | 29                           | 57.9                          | 56.1             | 58.2              | 28.9                              | 27.1             | 29.2              |
| <b>11:00AM</b> | 29                           | 61.2                          | 60.4             | 60.6              | 32.2                              | 31.4             | 31.6              |
| <b>12:00PM</b> | 29                           | 63.5                          | 65.2             | 64.7              | 34.5                              | 36.2             | 35.7              |
| <b>01:00PM</b> | 29                           | 71.4                          | 69.6             | 69.2              | 42.4                              | 40.6             | 40.2              |

|                |    |      |      |      |      |      |      |
|----------------|----|------|------|------|------|------|------|
| <b>02:00PM</b> | 29 | 70.8 | 68.7 | 68.1 | 41.8 | 39.7 | 39.1 |
| <b>03:00PM</b> | 29 | 60.7 | 67.5 | 66.3 | 31.7 | 38.5 | 37.3 |

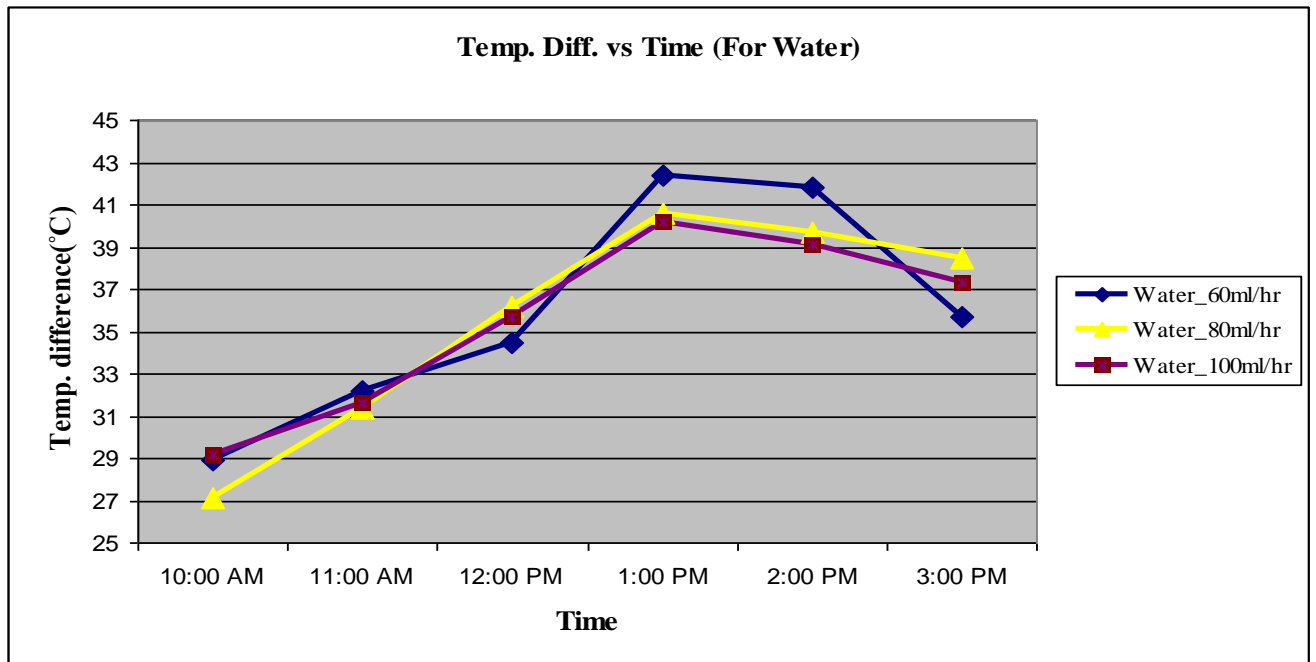


**Fig 5.2: Variation in temp. difference w.r.t time at different mass flow rates**

From Fig 5.2 it is observed clearly that as the Mass flow rate is decreasing the temperature difference is increasing and this may be due to the reason that at lower mass flow rate more amount of heat is being absorbed by water.

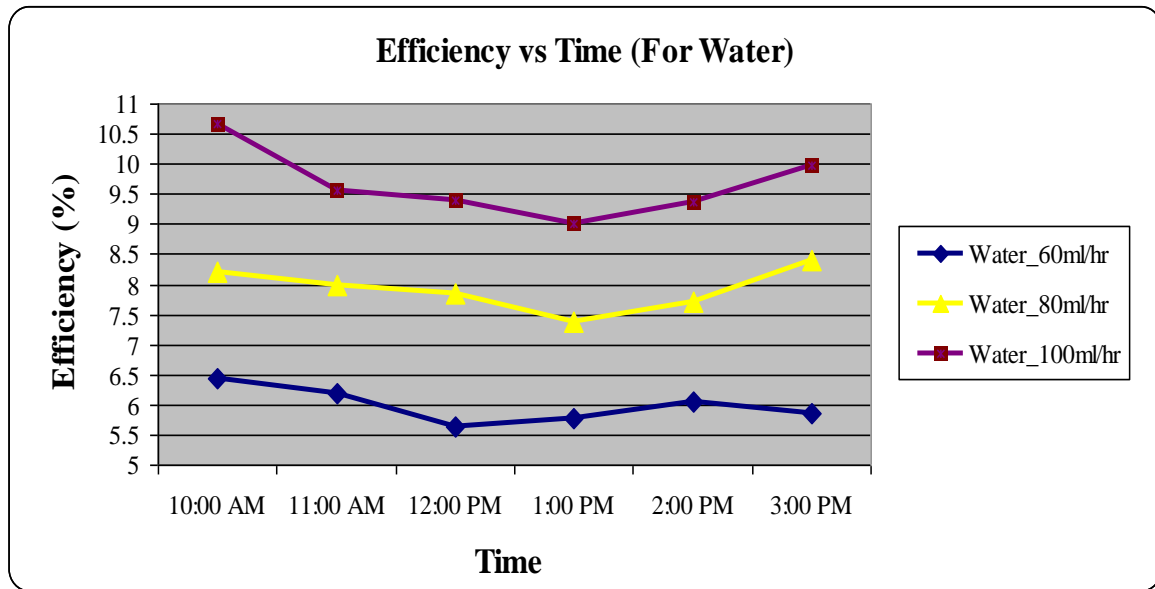


**Fig 5.3: Collector efficiency for water w.r.t time at different mass flow rates**

From Fig 5.3 it is observed clearly that as the mass flow rate increases efficiency increases, this may be due to the higher value of the mass flow rate and minimum efficiency is reported at 1:00 pm because at that time the value of global solar irradiation is maximum.

**Table 5.5: Efficiency of collector using water (For different mass flow rates)**

| Time    | TotalsolarRadiation 'W' |          |          | Heat Absorbed 'W' |           |            | Efficiency ' $\eta$ ' % |           |            |
|---------|-------------------------|----------|----------|-------------------|-----------|------------|-------------------------|-----------|------------|
|         | 5/5/2012                | 6/5/2012 | 7/5/2012 | 60(ml/hr)         | 80(ml/hr) | 100(ml/hr) | 60(ml/hr)               | 80(ml/hr) | 100(ml/hr) |
| 10:00AM | 33.984                  | 33.408   | 34.56    | 2.0167            | 2.5215    | 3.3961     | 6.450409                | 8.203906  | 10.68117   |
| 11:00AM | 39.456                  | 39.744   | 41.76    | 2.247             | 2.9215    | 3.6752     | 6.190164                | 7.989995  | 9.56605    |
| 12:00PM | 46.368                  | 46.656   | 48.096   | 2.4075            | 3.3682    | 4.15121    | 5.64365                 | 7.84698   | 9.383633   |
| 01:00PM | 55.584                  | 55.584   | 56.448   | 2.9588            | 3.7776    | 4.675      | 5.785994                | 7.387174  | 9.002899   |
| 02:00PM | 52.416                  | 52.128   | 52.704   | 2.9169            | 3.6938    | 4.5475     | 6.048809                | 7.702195  | 9.378671   |
| 03:00PM | 46.2528                 | 46.368   | 47.232   | 2.2121            | 3.5822    | 4.3381     | 5.19851                 | 8.397377  | 9.983329   |

**5.1.2 Performance evaluation of collector using Al<sub>2</sub>O<sub>3</sub>-H<sub>2</sub>O based nanofluid with  $\phi_p=0.05\%$**

For Al<sub>2</sub>O<sub>3</sub>( $\phi_p=0.05\%$ )Nanofluid

Density of Base fluid(Water),  $\rho_f=1000\text{Kg/m}^3$

Particle Density of Al<sub>2</sub>O<sub>3</sub> Nanoparticle,  $\rho_p =3965 \text{ Kg/m}^3$

Density of Nanofluid,  $\rho_{\text{eff}} = 1148.25 \text{ Kg/m}^3$

Specific Heat of Base fluid (water),  $C = 4.187 \text{ KJ/KgK}$

Specific Heat of Al<sub>2</sub>O<sub>3</sub> Nanoparticle,  $C_p = 1.046 \text{ KJ/KgK}$

Specific Heat of Al<sub>2</sub>O<sub>3</sub> Nanofluid,  $C_{\text{eff}} = 3.644 \text{ KJ/KgK}$

**Table 5.6: Mass Flow Rate**

| Vol. flow rate(ml/hr) | Mass flow rate(Kg/Sec)  |
|-----------------------|-------------------------|
| 60                    | $1.9138 \times 10^{-5}$ |
| 80                    | $2.5517 \times 10^{-5}$ |
| 100                   | $3.1896 \times 10^{-5}$ |

**Table 5.7: Temperature readings for Al<sub>2</sub>O<sub>3</sub> nanofluid ( $\phi_p = 0.05\%$ )**

| Time           | Temperature inlet(°C) | Temperature outlet(°C) |           |            | Temperature Difference(°C) |           |            |
|----------------|-----------------------|------------------------|-----------|------------|----------------------------|-----------|------------|
|                |                       | 60(ml/hr)              | 80(ml/hr) | 100(ml/hr) | 60(ml/hr)                  | 80(ml/hr) | 100(ml/hr) |
| <b>10:00AM</b> | 29                    | 61.2                   | 56.5      | 52.3       | 32.2                       | 27.5      | 23.3       |

|                |    |      |      |      |      |      |      |
|----------------|----|------|------|------|------|------|------|
| <b>11:00AM</b> | 29 | 64.4 | 63.1 | 59.6 | 35.4 | 34.1 | 30.6 |
| <b>12:00PM</b> | 29 | 68.7 | 65.9 | 65.3 | 39.7 | 36.9 | 36.3 |
| <b>01:00PM</b> | 29 | 70.7 | 68.3 | 69.2 | 41.7 | 39.3 | 40.2 |
| <b>02:00PM</b> | 29 | 66.7 | 67.2 | 64.4 | 37.7 | 38.2 | 35.4 |
| <b>03:00PM</b> | 29 | 65.3 | 64.4 | 55.3 | 36.3 | 35.4 | 26.3 |

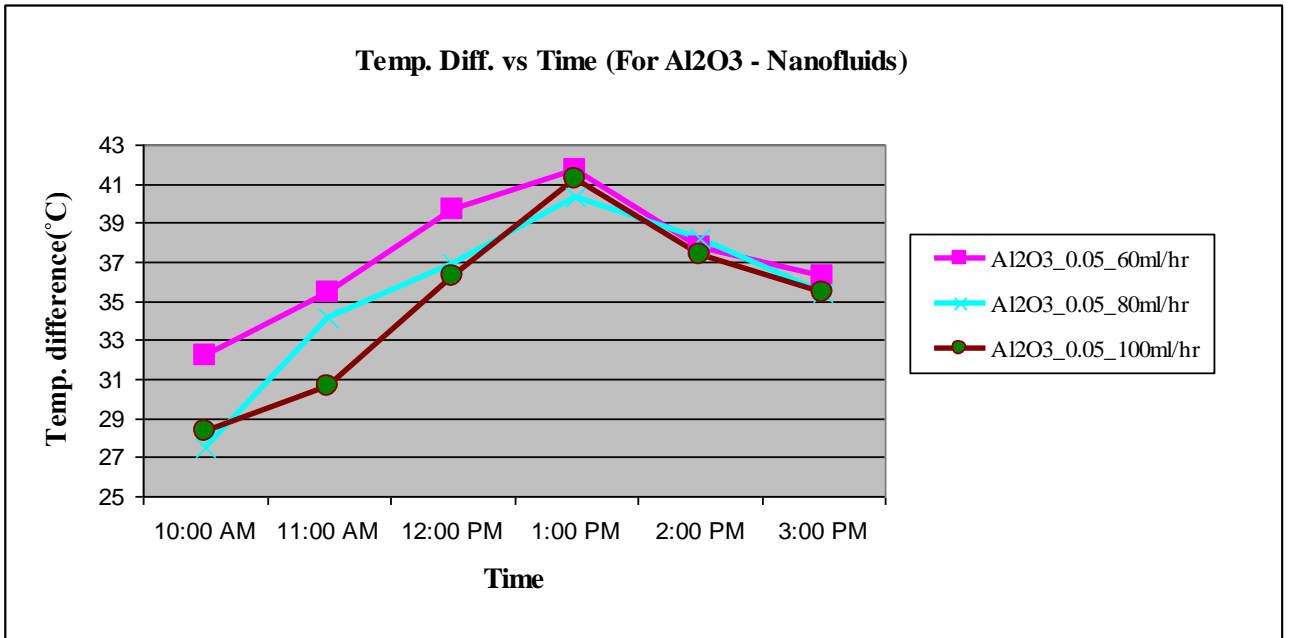


**Fig 5.4: Variation in temp. difference w.r.t time at different mass flow rates**

From Fig 5.4 shows clearly that for nanofluid as the mass flow rate increases at same volumetric concentration, temperature difference decreases. Maximum temperature difference is found in 60ml/hr mass flow rate.

**Table 5.8: Efficiency for collector using Al<sub>2</sub>O<sub>3</sub> nanofluid,  $\phi_P = 0.05\%$ , (For different mass flow rate)**

| Time    | Total Solar Radiation 'W' |         |         | Heat Absorbed 'W' |           |            | Efficiency ' $\eta$ ' % |           |            |
|---------|---------------------------|---------|---------|-------------------|-----------|------------|-------------------------|-----------|------------|
|         | 27/5/12                   | 28/5/12 | 29/5/12 | 60(ml/hr)         | 80(ml/hr) | 100(ml/hr) | 60(ml/hr)               | 80(ml/hr) | 100(ml/hr) |
| 10:00AM | 36.288                    | 32.544  | 33.984  | 2.2459            | 2.5575    | 2.7086     | 6.7274                  | 8.5419    | 9.6441     |
| 11:00AM | 42.912                    | 38.592  | 40.032  | 2.4691            | 3.1713    | 3.5572     | 6.2543                  | 8.9321    | 9.6587     |
| 12:00PM | 48.096                    | 45.504  | 47.0016 | 2.7690            | 3.4317    | 4.2198     | 6.2580                  | 8.0446    | 9.7589     |
| 01:00PM | 57.312                    | 53.856  | 55.0656 | 2.9085            | 3.6549    | 4.6732     | 5.5163                  | 7.3140    | 10.2554    |
| 02:00PM | 48.672                    | 49.6512 | 47.232  | 2.6295            | 3.5526    | 4.1152     | 5.8724                  | 7.7773    | 9.4705     |
| 03:00PM | 45.504                    | 45.0432 | 43.7184 | 2.5319            | 3.2922    | 3.0573     | 6.0480                  | 7.9445    | 7.6014     |

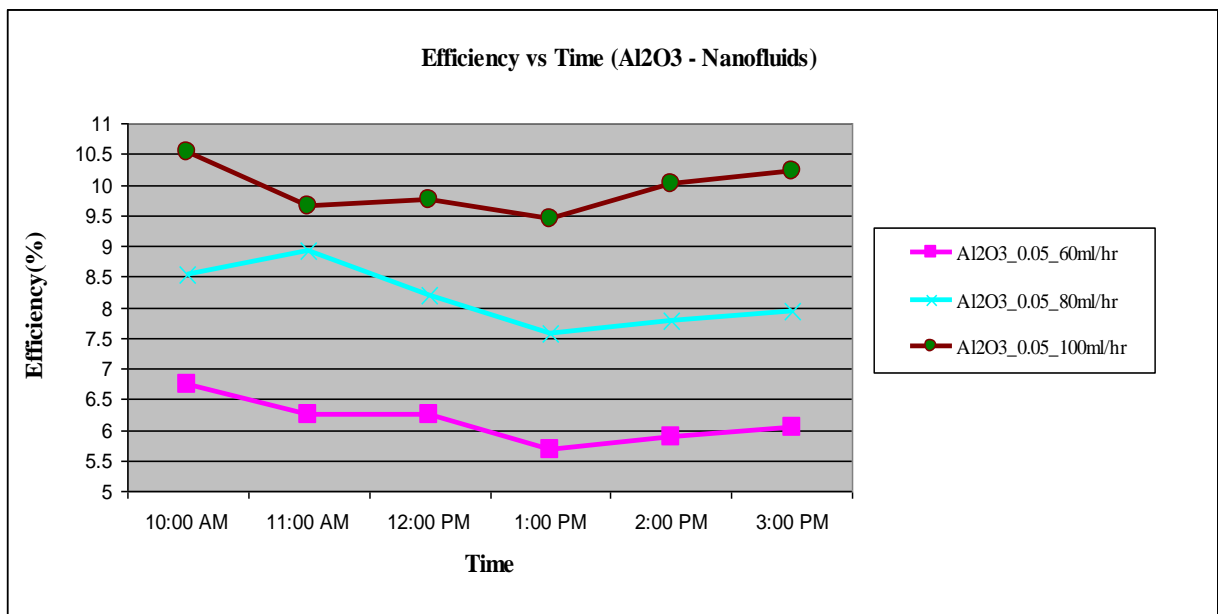


**Fig 5.5: Variation in collector efficiency w.r.t time at different mass flow rates for nanofluid**

From Fig 5.5 shows clearly that for higher mass flow rate efficiency is higher. At 1 pm efficiency is minimum in all cases because the value of  $G_T$  increases much faster than the heat gained by the collector.

### 5.1.3 Performance evaluation of solar collector using Al<sub>2</sub>O<sub>3</sub>-H<sub>2</sub>O Based nanofluids( $\phi=0.005\%$ )

For Al<sub>2</sub>O<sub>3</sub> ( $\phi_P = 0.005\%$ ) Nanofluid

Density of Base fluid (water),  $\rho_f = 1000 \text{ kg/m}^3$

Particle Density of Al<sub>2</sub>O<sub>3</sub> nanoparticle,  $\rho_P = 3965 \text{ kg/m}^3$

Density of Nanofluid,  $\rho_{\text{eff}} = 1014.825 \text{ Kg/m}^3$

Specific Heat of Base fluid (water),  $C = 4.187 \text{ KJ/KgK}$

Specific Heat of Al<sub>2</sub>O<sub>3</sub> nanoparticle,  $C_P = 1.046 \text{ KJ/KgK}$

Specific Heat of Al<sub>2</sub>O<sub>3</sub> nanofluid,  $C_{\text{eff}} = 4.1256 \text{ KJ/KgK}$

**Table 5.9: Mass flow Rate**

| Vol. flow rate(ml/hr) | Mass flow rate(Kg/sec) |
|-----------------------|------------------------|
| 60                    | $1.691 \times 10^{-5}$ |
| 80                    | $2.255 \times 10^{-5}$ |
| 100                   | $2.819 \times 10^{-5}$ |

**Table 5.10: Temperature readings for Al<sub>2</sub>O<sub>3</sub> - H<sub>2</sub>O based nanofluid ( $\phi_P = 0.005\%$ )**

| Time           | Temperature Inlet(°C) | Temperature outlet(°C) |           |            | Temperature difference(°C) |           |            |
|----------------|-----------------------|------------------------|-----------|------------|----------------------------|-----------|------------|
|                |                       | 60(ml/hr)              | 80(ml/hr) | 100(ml/hr) | 60(ml/hr)                  | 80(ml/hr) | 100(ml/hr) |
| <b>10:00AM</b> | 29                    | 58.8                   | 55.3      | 56.2       | 29.8                       | 26.3      | 27.2       |
| <b>11:00AM</b> | 29                    | 62.4                   | 62.5      | 60.4       | 33.4                       | 33.5      | 31.4       |
| <b>12:00PM</b> | 29                    | 65.7                   | 66.7      | 63.5       | 36.7                       | 37.7      | 34.5       |
| <b>01:00PM</b> | 29                    | 69.5                   | 69.3      | 67.9       | 40.5                       | 40.3      | 38.9       |
| <b>02:00PM</b> | 29                    | 67.3                   | 66.3      | 66.2       | 38.3                       | 37.3      | 37.2       |
| <b>03:00PM</b> | 29                    | 65.4                   | 64.7      | 64.3       | 36.4                       | 35.7      | 35.3       |

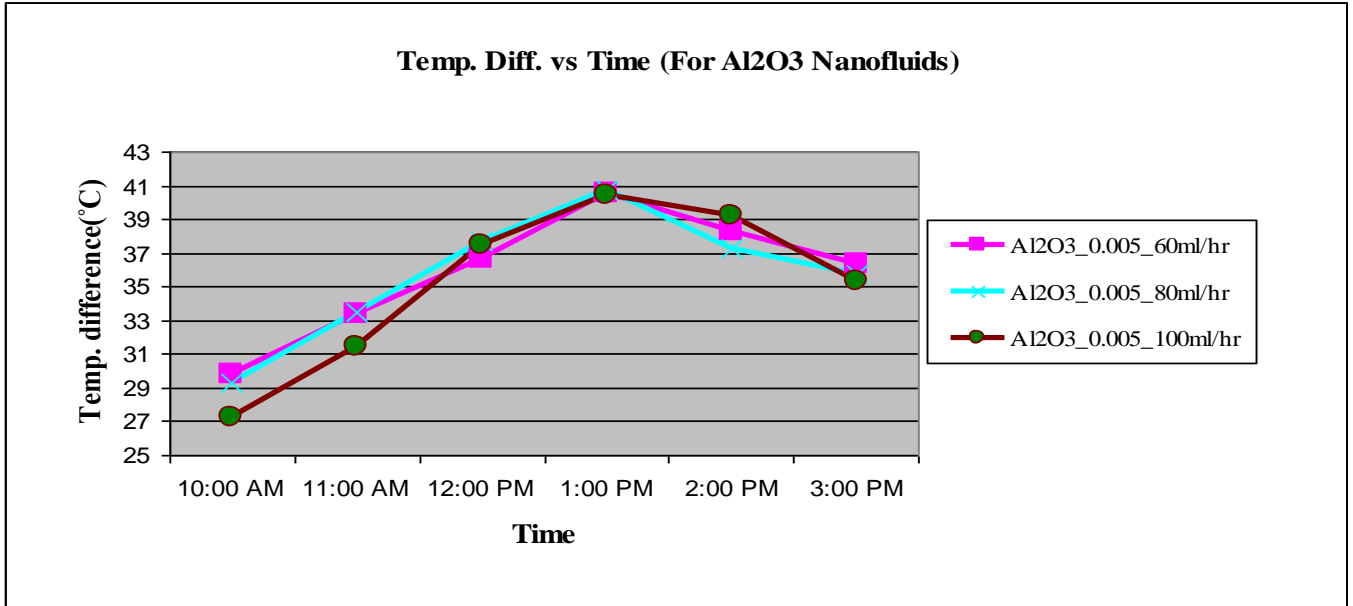


**Fig 5.6: Variation in temperature difference w.r.t time at different mass flow rates for Al<sub>2</sub>O<sub>3</sub> nanofluid**

From Fig 5.6 it is clearly observed that the temperature difference is increasing with low mass flow rates before 11 am .After 12 pm temp.difference is almost same , this may be due to the reason that at higher mass flow rate increase in heat gain is more compared to heat gain due to low mass flow rate.

**Table 5.11: Efficiency for collector using Al<sub>2</sub>O<sub>3</sub> nanofluid,  $\phi_p = 0.005\%$ , (For different mass flow rates)**

| Time    | Total Solar Radiation 'W' |        |        | Heat absorbed 'W' |           |            | Efficiency ' $\eta$ ' % |           |            |
|---------|---------------------------|--------|--------|-------------------|-----------|------------|-------------------------|-----------|------------|
|         | 2/6/12                    | 4/6/12 | 7/6/12 | 60(ml/hr)         | 80(ml/hr) | 100(ml/hr) | 60(ml/hr)               | 80(ml/hr) | 100(ml/hr) |
| 10:00AM | 33.868                    | 33.984 | 33.696 | 2.0794            | 2.4469    | 3.1633     | 6.6735                  | 7.8264    | 10.4728    |
| 11:00AM | 39.916                    | 39.974 | 41.702 | 2.3306            | 3.1168    | 3.6518     | 6.3464                  | 8.5864    | 9.7887     |
| 12:00PM | 46.656                    | 46.368 | 47.232 | 2.5609            | 3.5076    | 4.0123     | 5.9662                  | 8.2225    | 9.2336     |
| 1:00 PM | 53.856                    | 54.432 | 55.296 | 2.8260            | 3.7495    | 4.5240     | 5.7037                  | 7.4874    | 9.1798     |
| 02:00PM | 47.462                    | 49.305 | 49.305 | 2.6725            | 3.4703    | 4.326      | 6.1205                  | 7.6505    | 9.5375     |
| 03:00PM | 45.792                    | 44.64  | 44.064 | 2.5399            | 3.3215    | 4.1053     | 6.0291                  | 8.0877    | 10.1270    |

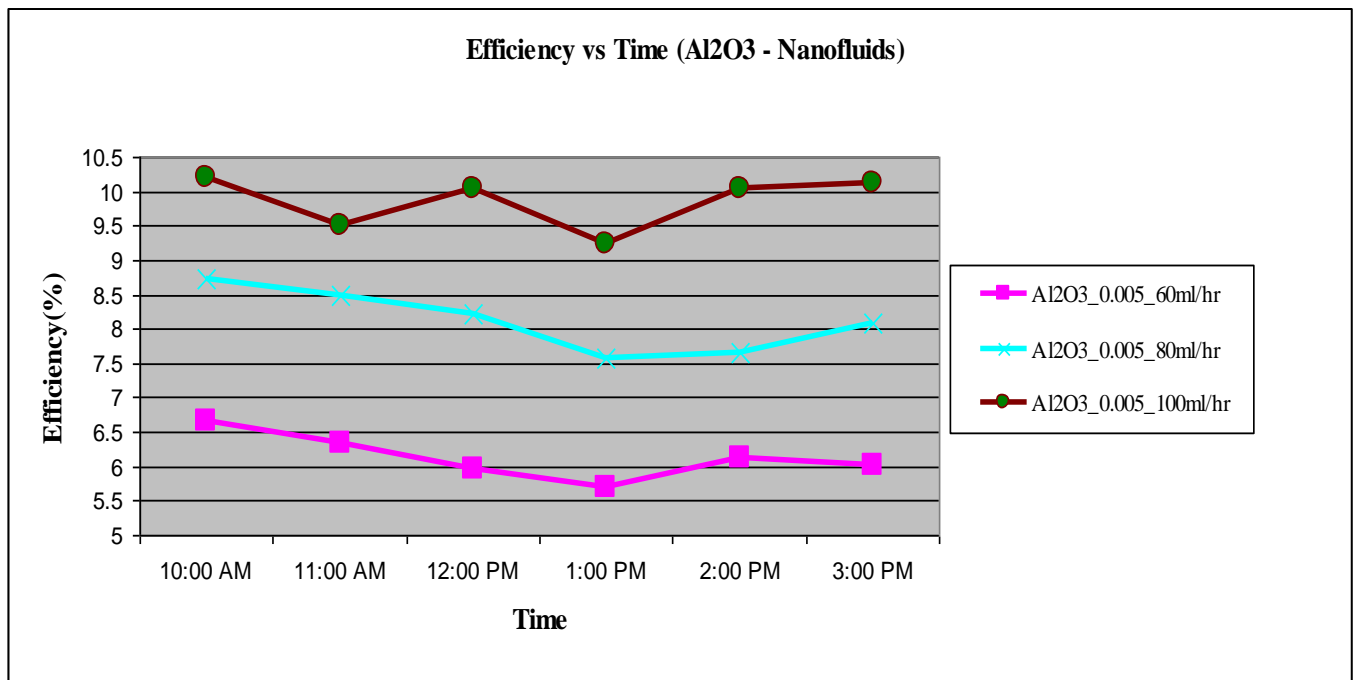


**Fig 5.7: variation in collector efficiency w.r.t time at different mass flow rates**

From Fig 5.7 it is observed that at higher mass flow rates the efficiency is higher than low mass flow rates, this may be due to the higher value of mass flow rate. The value of temperature difference is also almost constant between 12 pm to 2 pm.

#### 5.1.4 Comparison charts of solar collector

### 5.1.4.1 Comparison charts between water and Al<sub>2</sub>O<sub>3</sub> nanofluid ( $\phi_P = 0.05\%$ )

#### Temperature Difference comparison

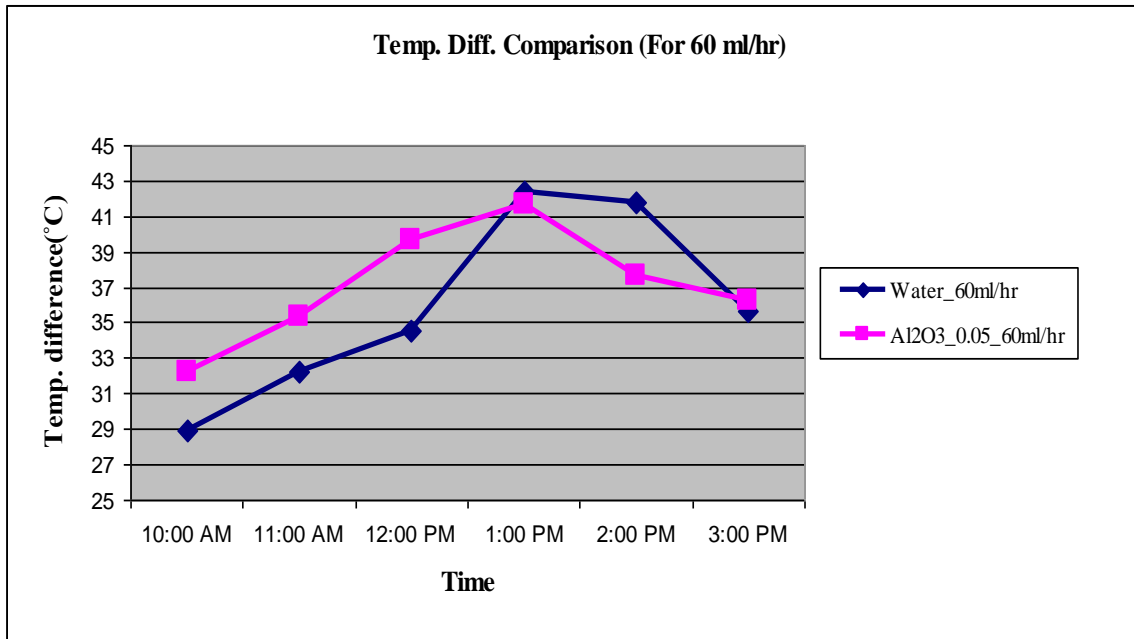


Fig 5.8: Variation in temp. diff. w.r.t time for water and Al<sub>2</sub>O<sub>3</sub> nanofluid for 60ml/hr

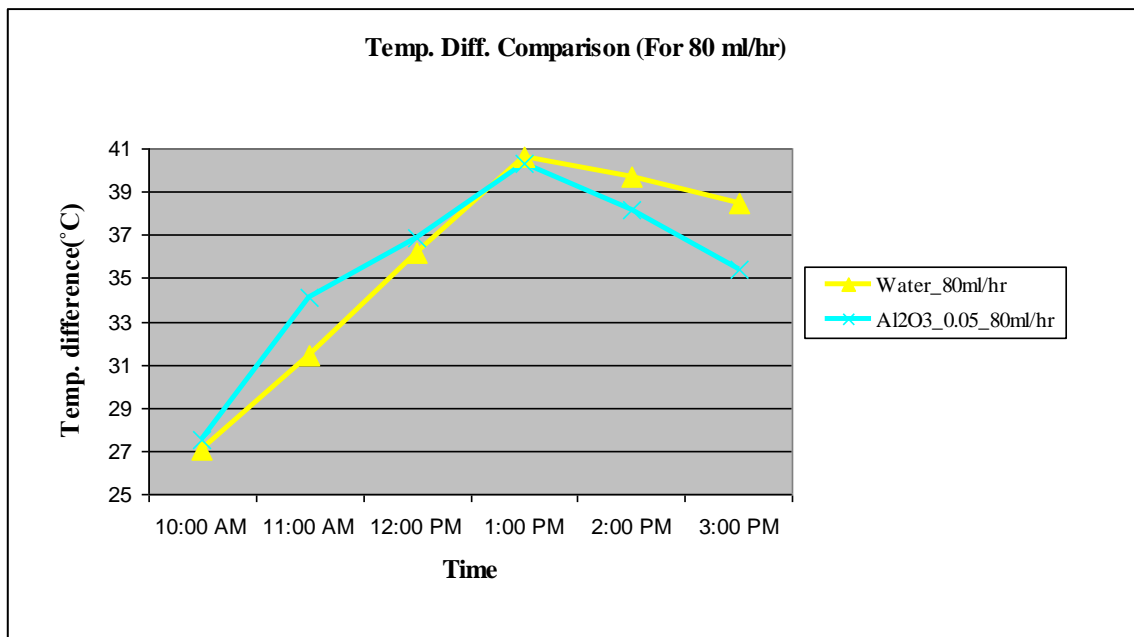
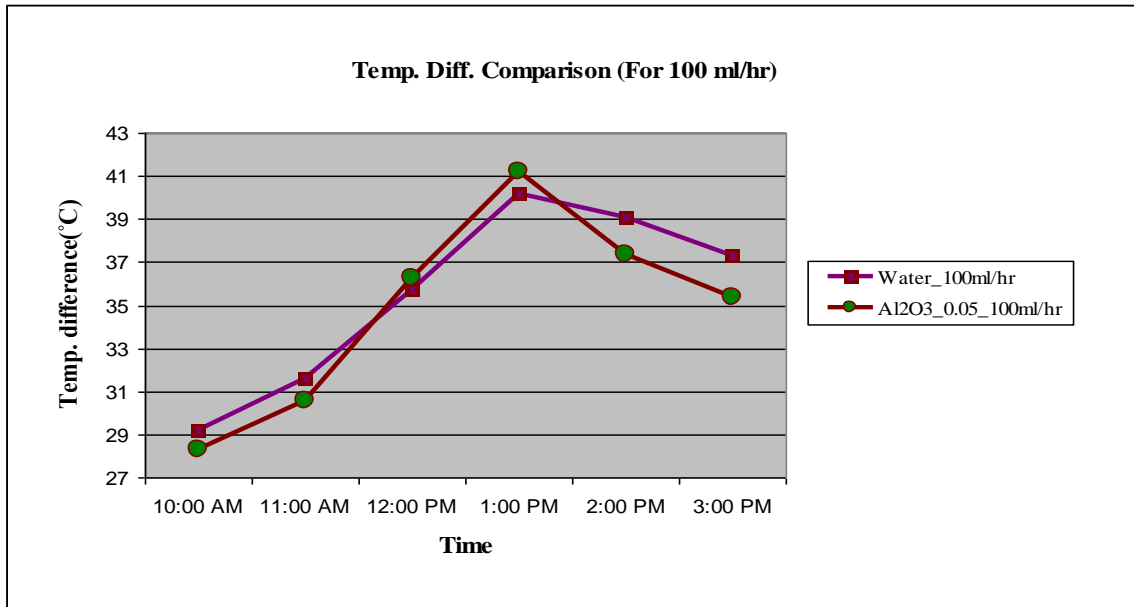


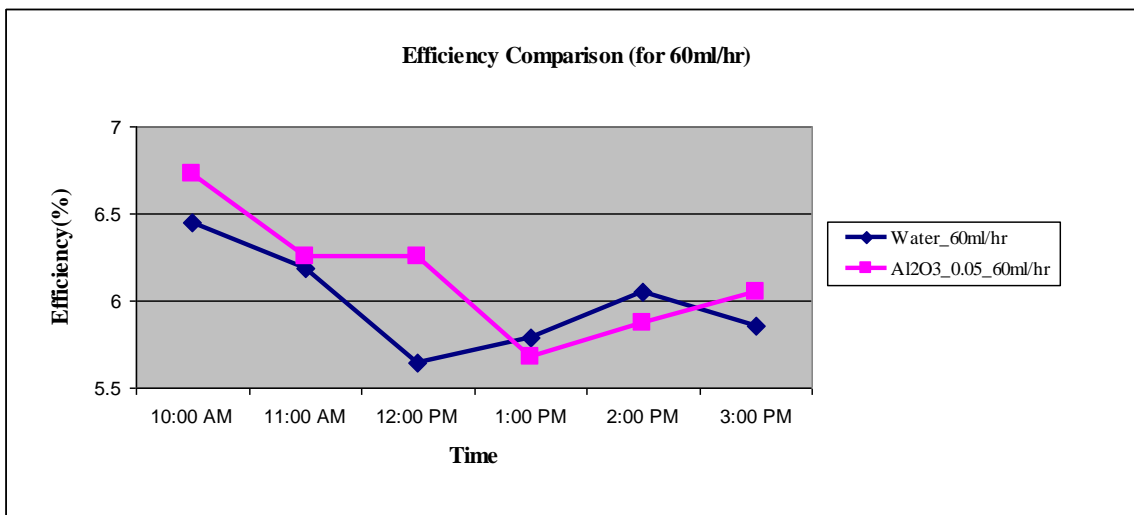
Fig 5.9: Variation in temp. diff. w.r.t time for water and Al<sub>2</sub>O<sub>3</sub> nanofluid for 80ml/hr



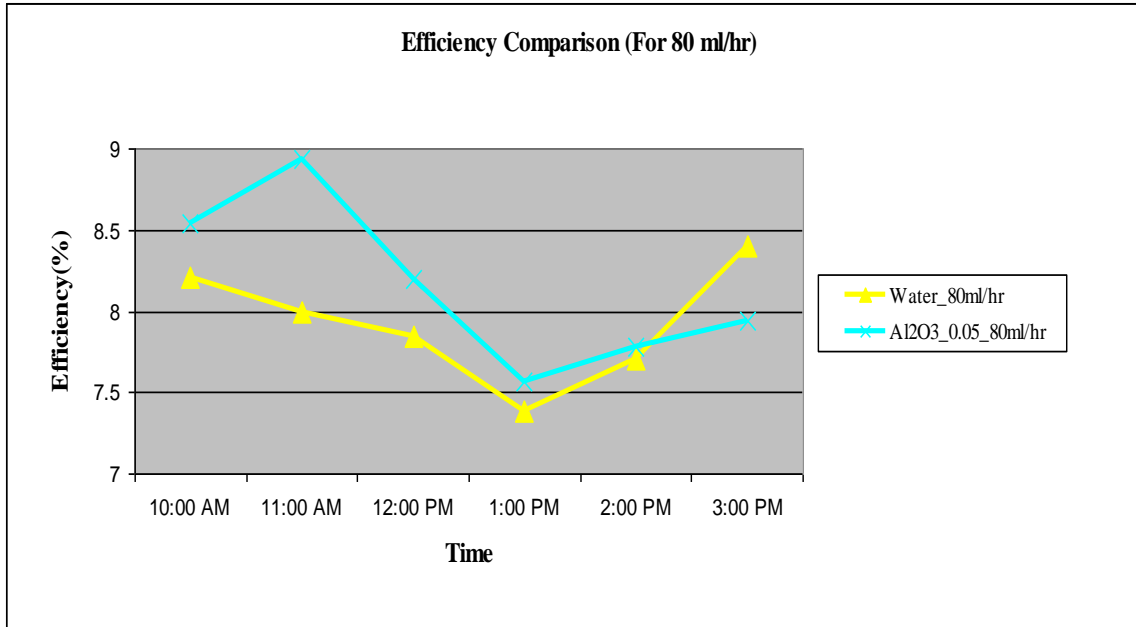
**Fig 5.10: Variation in temperature difference w.r.t time for water and Al<sub>2</sub>O<sub>3</sub> nanofluid for 100ml/hr**

Fig 5.8,5.9,5.10 show that Al<sub>2</sub>O<sub>3</sub> nanofluid has higher temperature difference before 12 pm as compared to water but after 12 pm the value of water rises slightly and this may be due to the reason that the fall in temperature in case of nanofluid is more rapid as compared to water.

### Efficiency Comparison



**Fig 5.11: Variation in collector efficiency w.r.t time for water and Al<sub>2</sub>O<sub>3</sub> nanofluid for 60ml/hr**



**Fig 5.12: Variation in collector efficiency w.r.t time for water and Al<sub>2</sub>O<sub>3</sub> nanofluid for 80ml/hr**

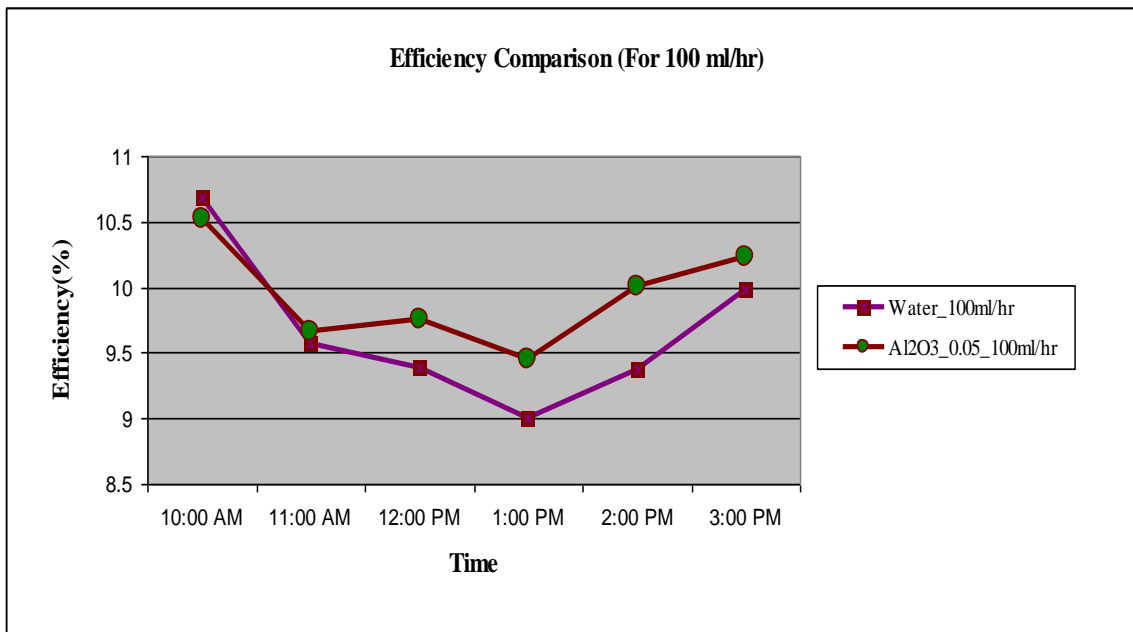


**Fig 5.13: Variation in collector efficiency w.r.t time for water and Al<sub>2</sub>O<sub>3</sub> nanofluid for 100ml/hr**

Fig 5.11,5.12,5.13 show that the efficiency of the collector is always slightly more than water and this rise is due to the more amount of heat gained by nanofluid as compared to water.

### 5.1.4.2 Comparison charts water and Al<sub>2</sub>O<sub>3</sub> nanofluid( $\phi_P = 0.005\%$ )

#### Temperature difference comparison

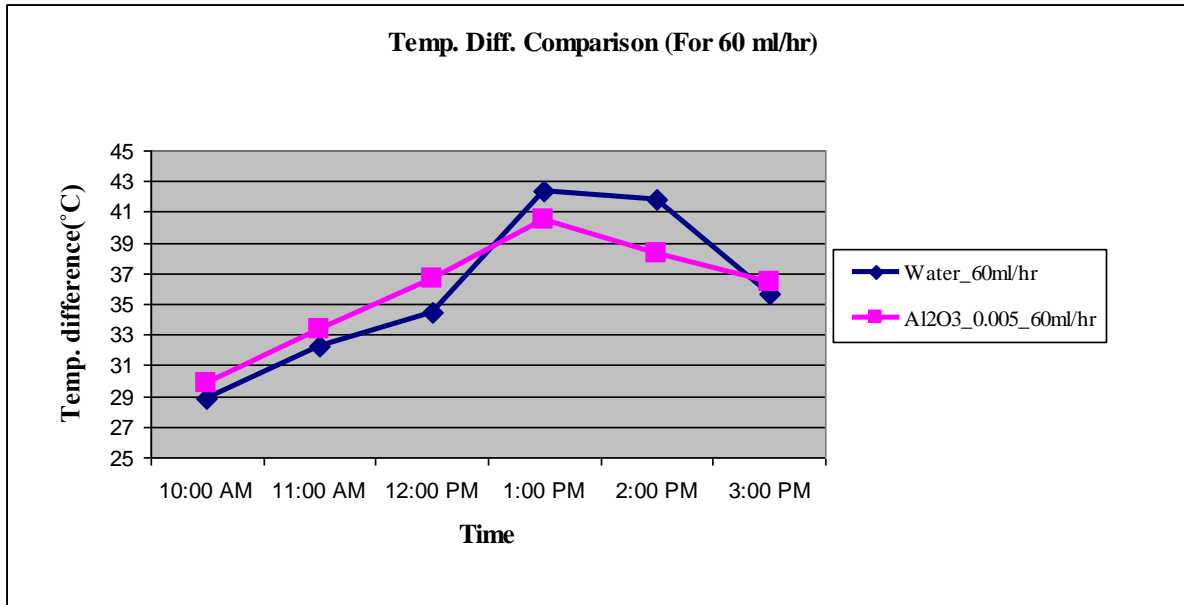


Fig 5.14: Variation in temperature difference w.r.t time for water and Al<sub>2</sub>O<sub>3</sub> nanofluid for 60ml/hr

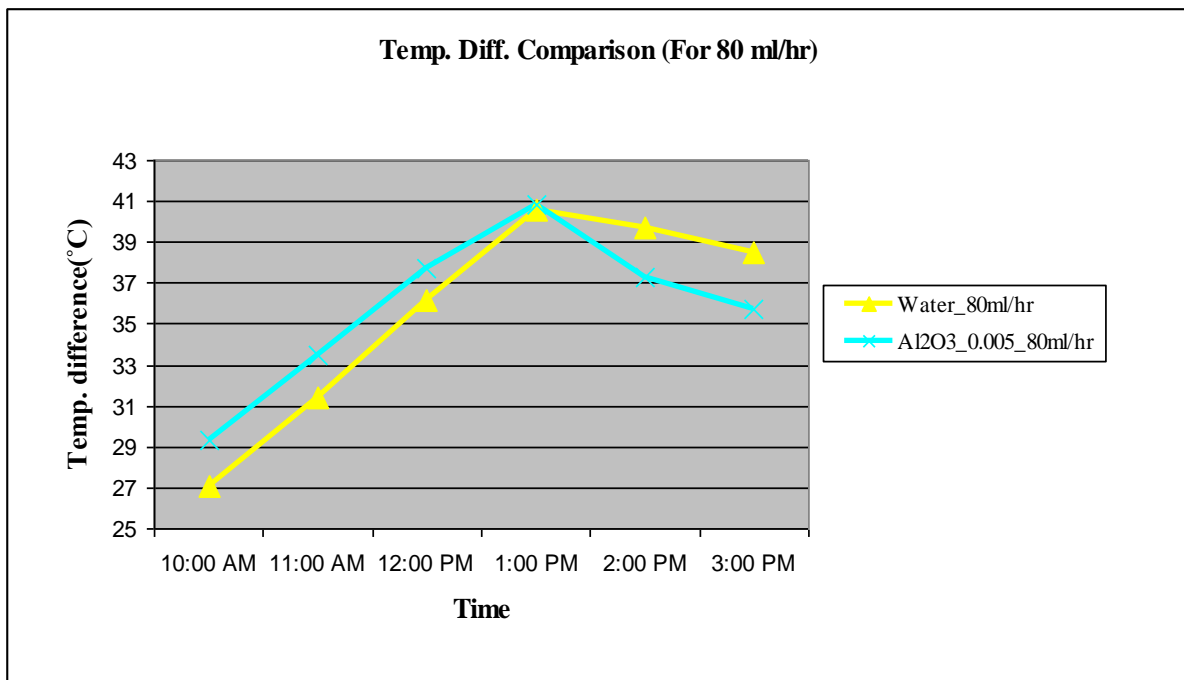
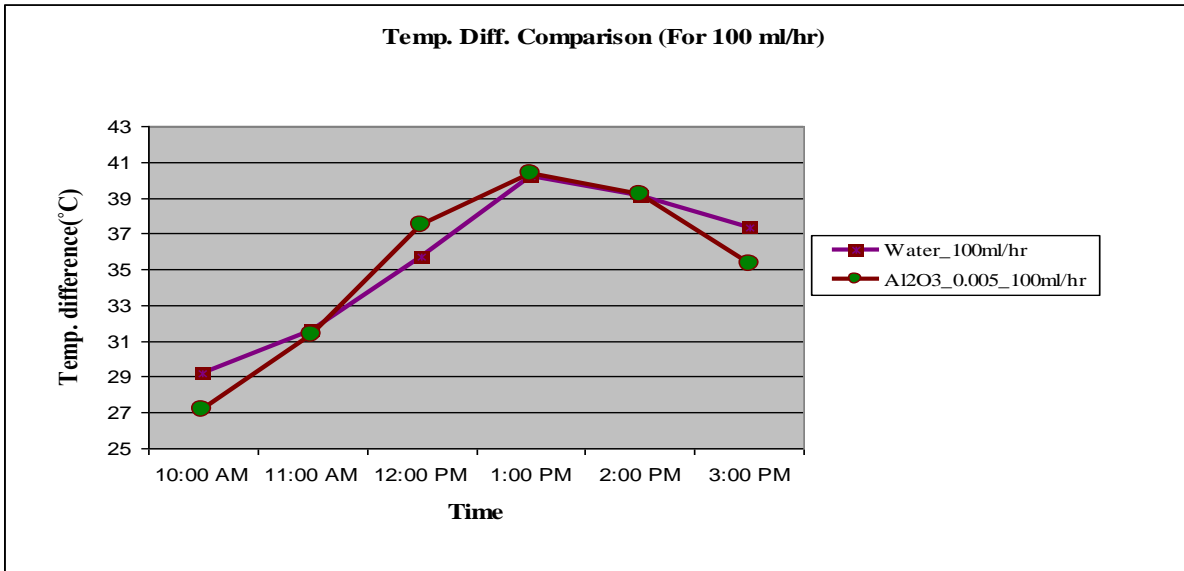


Fig 5.15: Variation in temperature difference w.r.t time for water and Al<sub>2</sub>O<sub>3</sub> nanofluid for 80ml/hr



**Fig 5.16: Variation in temp. diff. w.r.t time for water and Al<sub>2</sub>O<sub>3</sub> nanofluid for 100ml/hr**

From fig 5.14,5.15,5.16 it is observed that at different time intervals the temperature difference is varying and in most of the cases the temperature difference for Al<sub>2</sub>O<sub>3</sub> is higher than water. This is because of the higher heat absorption capacity of the nanofluids as compared to water.

### Efficiency comparison

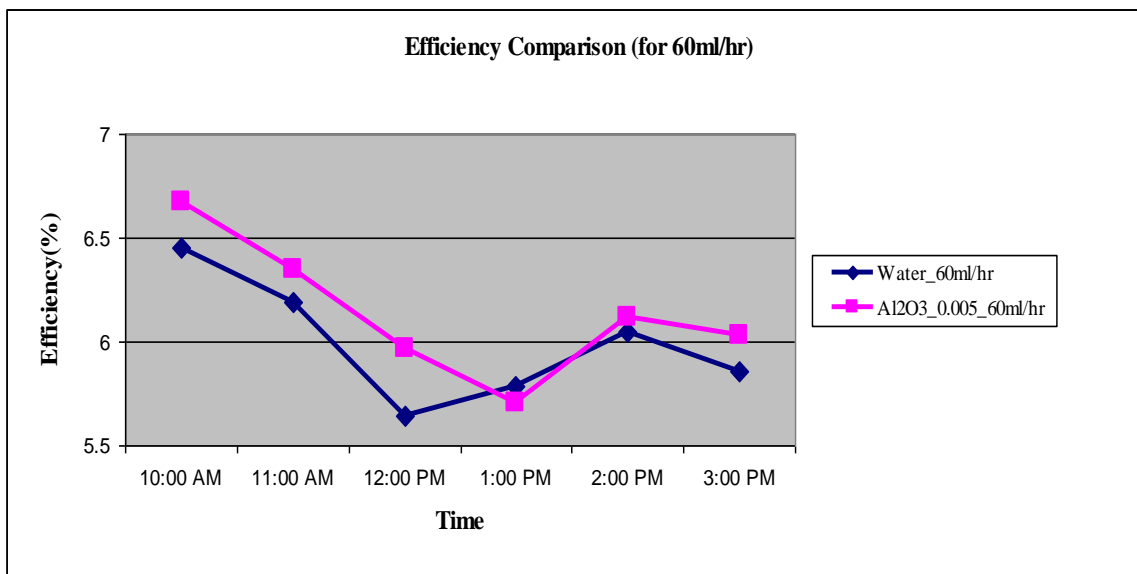


**Fig 5.17: Variation in collector efficiency w.r.t time for water and Al<sub>2</sub>O<sub>3</sub> nanofluid for 60ml/hr**

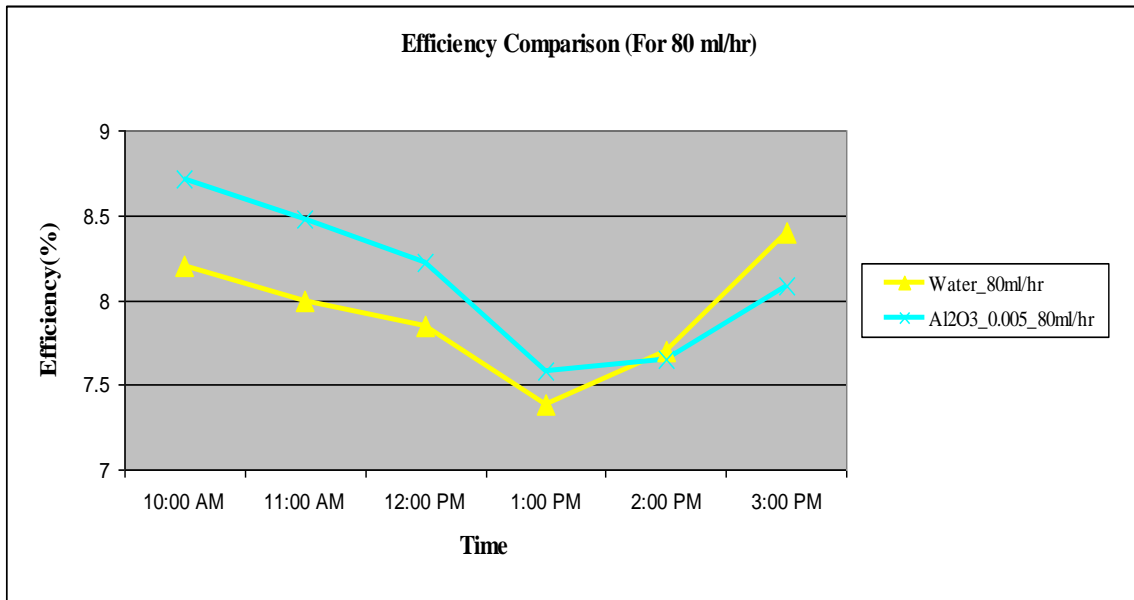


**Fig 5.18: Variation in collector efficiency w.r.t time for water and Al<sub>2</sub>O<sub>3</sub> nanofluid for 80ml/hr**

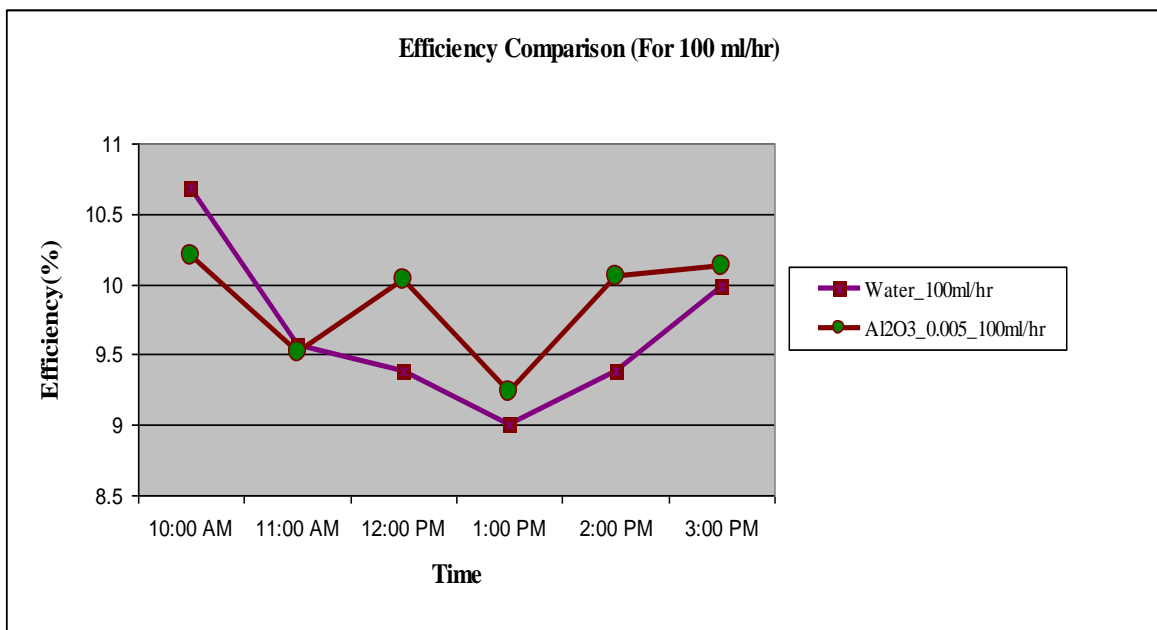


**Fig 5.19: Variation in collector efficiency w.r.t time for water and Al<sub>2</sub>O<sub>3</sub> nanofluid for 100ml/hr**

From these plots it can be concluded that efficiency of the collector using nanofluid is higher than as compared to water. The efficiency is low at 01:00 PM this is because of the higher value global solar irradiation. Fig 5.19 shows that there is increase and decrease of the efficiency, this is due to the windy conditions prevailing that day.

### 5.1.4.3: Comparison charts between $\text{Al}_2\text{O}_3(\phi_P=.05\%)$ and $\text{Al}_2\text{O}_3(\phi_P=.005\%)$ :

#### Temperature Difference Comparison:

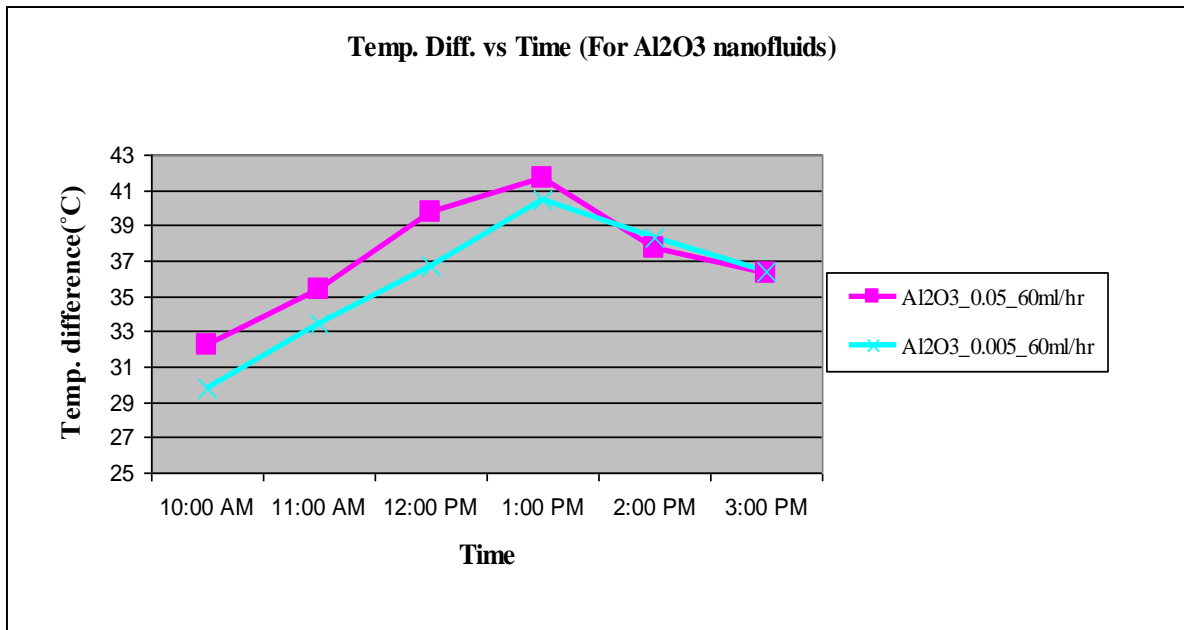


**Fig 5.20: Variation in temp. diff. w.r.t time for different volumetric concentrations for 60ml/hr**

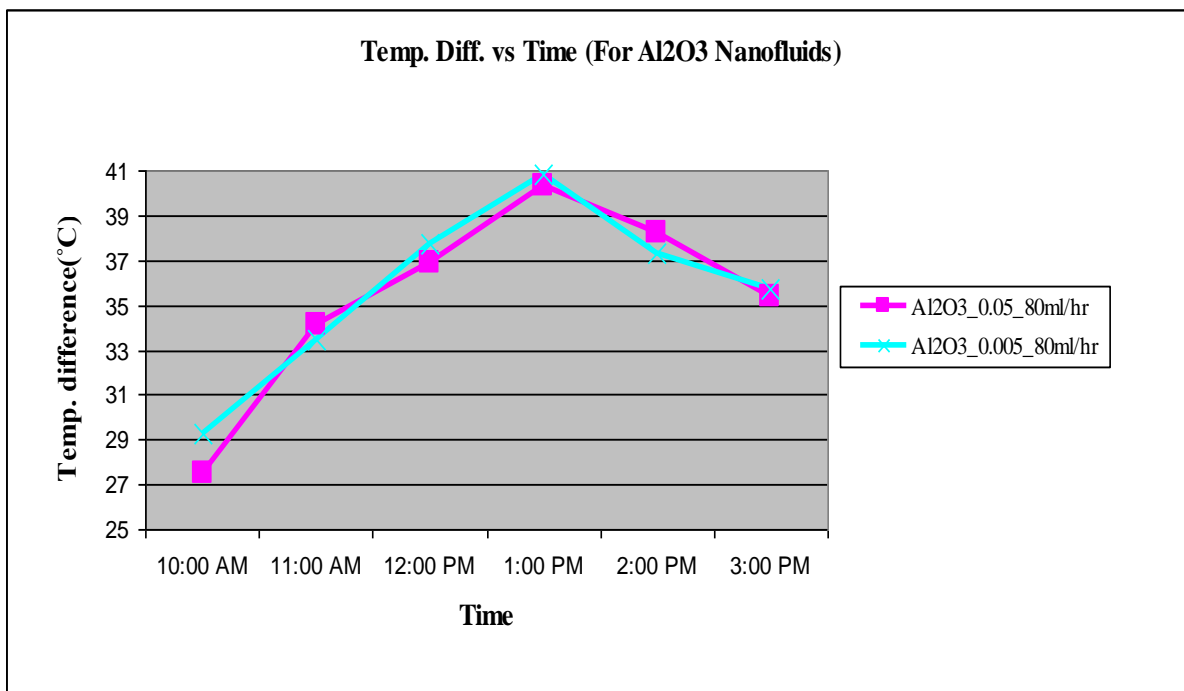


**Fig 5.21: Variation in temp. diff. w.r.t time for different volumetric concentrations for 80ml/hr**

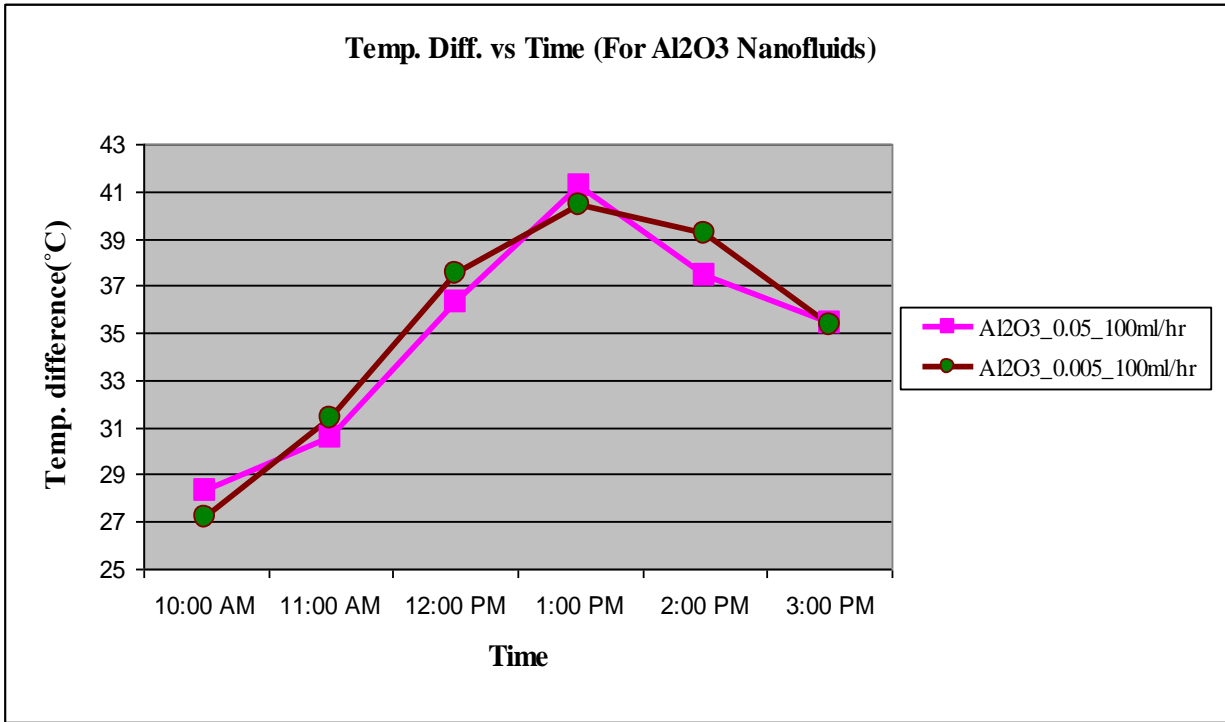


**Fig 5.22: Variation in temp. diff. w.r.t time for different volumetric concentrations for 100ml/hr**

From fig 5.20,5.21,5.22 it is clearly seen that the temperature difference in case of low volumetric concentration ( $\phi_p=0.005\%$ ) is slightly higher than the higher volumetric concentration ( $\phi_p=0.05\%$ ). This is because at higher volumetric concentration the problem of settling down of nanoparticles is more serious as compared to low volumetric concentration.

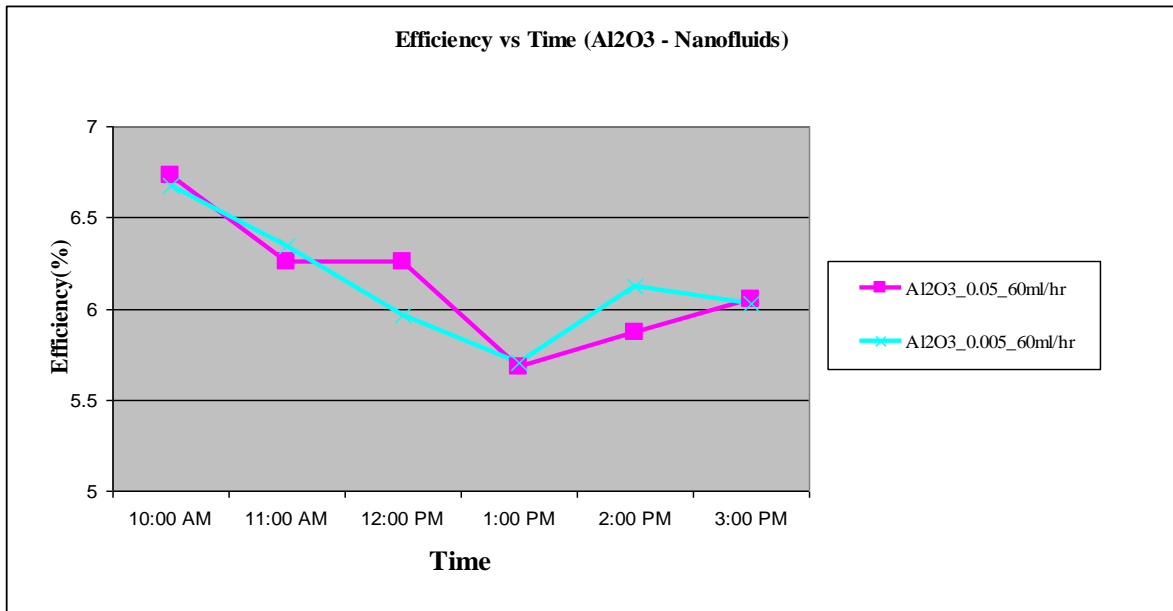


**Fig 5.23: Variation in collector efficiency w.r.t time for Al<sub>2</sub>O<sub>3</sub>( $\phi_P=.005$ ) and Al<sub>2</sub>O<sub>3</sub>( $\phi_P=.05$ ) nanofluids for 60ml/hr**

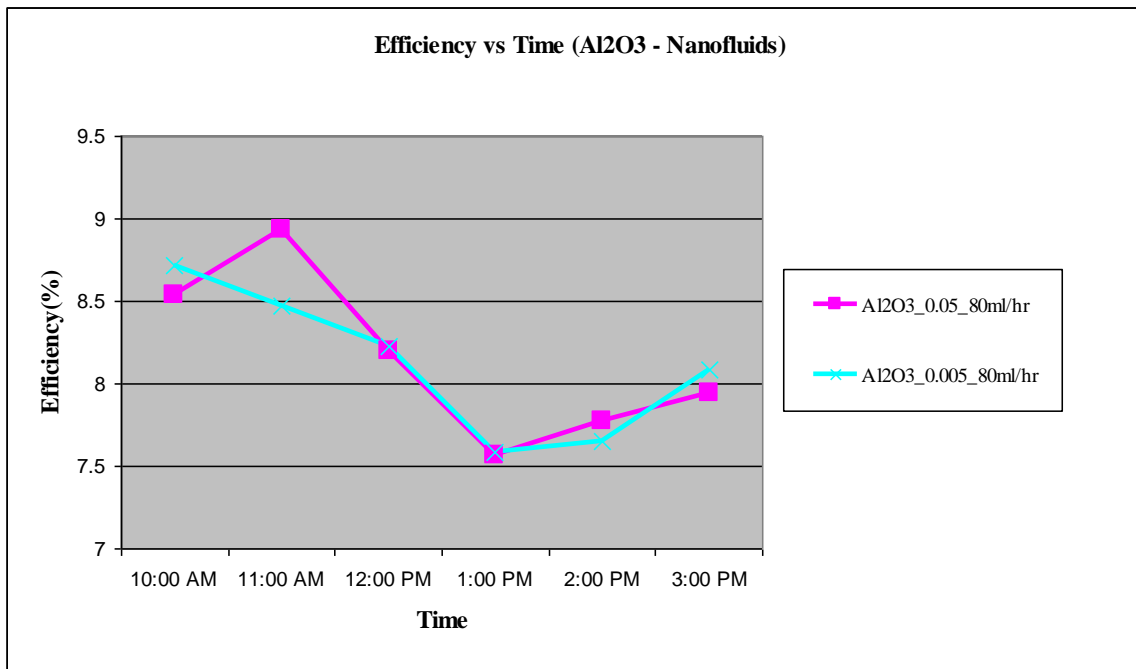


**Fig 5.24: Variation in collector efficiency w.r.t time for Al<sub>2</sub>O<sub>3</sub>( $\phi_P=.005$ ) and Al<sub>2</sub>O<sub>3</sub>( $\phi_P=.05$ ) nanofluids for 80ml/hr**



**Fig 5.25: Variation in collector efficiency w.r.t time for Al<sub>2</sub>O<sub>3</sub>( $\phi_P=.005$ ) and Al<sub>2</sub>O<sub>3</sub>( $\phi_P=.05$ ) nanofluids for 100ml/hr**

From fig 5.23,5.24,5.25 this can be observed that the efficiency of the collector in case of Al<sub>2</sub>O<sub>3</sub>( $\phi_P=.005\%$ ) is slightly higher than Al<sub>2</sub>O<sub>3</sub>( $\phi_P=.05\%$ ) because at higher volumetric concentration particle settling is a major problem and at lower volumetric concentration larger amount of heat is not gained properly.

### CONCLUSION AND FUTURE SCOPE

From the results obtained by performing the experiments, this can be concluded that

1. The efficiency of the collector increases upto 4-5% on an average as compared to water. This is due to the high thermal properties of the nanofluids.
2. At higher mass flow rate the temperature difference decreases but efficiency increases.
3. The efficiency is found minimum near 1 pm. This is due to the higher value of global solar irradiance.
4. When we compare two volumetric concentrations of nanofluids for same mass flow rate it is found that at higher volumetric concentration settling problems are more dominant. Hence, efficiency at lower volumetric concentration is slightly higher.
5. Higher efficiency can be obtained in case of nanofluids if the settling of the nanoparticles in the fluid is prevented.

There is a lot of scope for research in this area in future. Since study of Nanofluids is under initial stages so there is a lot of scope in development of nanofluids. The size, shape, material and volume fraction of nanoparticles play a very important role in the absorption of solar energy by nanofluids. If we have large availability of nanofluids the size of the collector can be increased. Due to high absorption characteristics of the nanofluids large amount of heat can be absorbed and this heat can be used for desired purposes. DASC is the new type of solar collectors which absorbs solar radiations volumetrically which helps in the enhancement of the efficiency. Also using Nanofluids in concentrated solar collectors we will be able to produce electricity but the problem lies in quantity of nanofluids . So, if we are able to produce large quantities of Nanofluids this problem can be overtaken.

## REFERENCES

---

- 1) Garg.H.P, Prakash.J, Solar Energy Fundamental and Applications, Tata McGraw Hill, ISBN 0-07-463631-6, Page(35,46,116), 1997.
- 2) Robert F, Ghassemi M, Alma C, Solar Energy -Renewable Energy and the Environment,CRC Press, ISBN : 978-1-4200-7566-3-90000.
- 3) Minardi.J.E, Chuan.H.N, Solar Energy, Page(17,18),1975.
- 4) Sukhatme S.P, Solar energy Fundamental and Applications, Tata Mcgraw Hill Publication, ISBN:0-07-451946-8, 1984.
- 5) Taylor A.R, Phelan E.P, Otanicar P.T, Walker A.C, Nguyen M,Trimble S, Ravi P, Applicability of Nanofluids in high flux solar collectors, Journal of Renewable and Sustainable Energy 3, 023104(2011).
- 6) Das.K.S, Choi.S.U.S, YU.W, Pradeep.T, Nanofluids science and Technology , ISBN: 978-0-470-07473-2, Page(1-30).
- 7) Choi S.U.S, Nanofluid Technology:Current Status and Future research, Energy Technology Division , Argonne National Laboratory, Sep28,1999.
- 8) Lee.S, Choi S.U.S, Li.S, Eastman J.A, Measuring Thermal conductivity of fluids containing oxide Nanoparticles ,ASME Journal Heat Transfer 1999;121:280-9.
- 9) Otanicar P.T, Pehlan E P, Prasher S.R, Rosengarten G, Taylor A.R, Nanofluid- based direct Absorption solar collector, Journal of Renewable and Sustainable Energy 2, 033102 (2010)
- 10) Tyagi.H, Phelan.P, Prasher.R, Predicted Efficiency of a Low-Temperature Nanofluid based Direct Absorption Solar Collector, Journal of Solar Energy, Vol.131 (2009).
- 11) Natrajan E, Sathish R, Role of Nanofluids in solar water heater , Springer-verlag London,(2008).

- 12) Han Z, Nanofluids with enhancement Thermal transport Properties, Department of Mechanical Engineering, University of Maryland at college park,(2008).
- 13) Trisakri v, Wongwises s, *Critical Review of Heat Transfer characteristics of nanofluids.*
- 14) Yousefi T, Veysi F, Shojaeizadeh E, Zinadini S, An experimental investigation on the effect of Al<sub>2</sub>O<sub>3</sub>-H<sub>2</sub>O Nanofluids on the efficiency of flat plate solar collector, *Journal of renewable energy* 39(2012)293-298.
- 15) Timofeeva V E, YU W, France M D, Singh D, Routbort L J, Nanofluids for heat transfer: An Engineering approach, *Nanoscale research Letters* ,6:182(2011).
- 16) Draft ASHRAE Standards, Proposed standards 77-93 , Third Public Review (May 2009).
- 17) Garg H.P, Prakash J, *Solar energy Fundamentals and Applications*, Tata McGraw Hill Publication, ISBN 0-07-463631-6, 1997.
- 18) Goswami D, Yogi, Kreith. Frank, Kreider, Jan F, *Principles of solar engineering*, 2nd edition, Taylor and Francis, Philadelphia, PA(2000).
- 19) Wang.X.Q, Mujumdar.A.S, Heat transfer characteristics of nanofluids: a review, *International Journal of Thermal Sciences* 46 (2007) 1 -19
- 20) Khanafer K, Vafai K, A Critical synthesis of thermophysical Characteristics of Nanofluids, *International Journal of Heat and Mass transfer*(Under Press), 2011.
- 21) Rai.G.D, *Solar energy utilization* , khanna publishers, New delhi(1996).
- 22) Pyranometer CMP-11 from Kipp & Zonen,

[http://users.du.se/~ffi/SERC/Hybrid/technical\\_data.htm](http://users.du.se/~ffi/SERC/Hybrid/technical_data.htm)

## ANNEXURE

---

### XRD of Purchased Sample of Nanoparticles:

|  |   |
|--|---|
| Dataset Name                             | SAMPLE-1 VIVEK VERMA  |
| File name                                | C:\X'Pert Data\MAY2012\SAMPLE-1 Vivek verma.xrdml   |
| Comment                                  | Configuration=Flat Sample Stage, Owner=jagtar, Creation date=6/11/2007 3:57:00 PM<br>Goniometer=PW3050/60 (Theta/Theta); Minimum step size 2Theta:0.001; Minimum step size Omega:0.001<br>Sample stage=PW3071/xx Bracket<br>Diffractometer system=XPERT-PRO<br>Measurement program=PU, Owner=jagtar, Creation date=4/15/2008 1:52:59 PM |
| Measurement Date / Time                  | 5/24/2012 3:42:13 PM  |
| Operator                                 | Panjab University   |
| Raw Data Origin                          | XRD measurement (*.XRDML)   |
| Scan Axis                                | Gonio   |
| Start Position [ $^{\circ}2\text{Th.}$ ] | 10.0084   |
| End Position [ $^{\circ}2\text{Th.}$ ]   | 99.9894   |
| Step Size [ $^{\circ}2\text{Th.}$ ]      | 0.0170  |
| Scan Step Time [s]                       | 25.1954   |
| Scan Type                                | Continuous  |

|                               |                  |
|-------------------------------|------------------|
| PSD Mode                      | Scanning         |
| PSD Length [°2 $\theta$ .]    | 2.12             |
| Offset [°2 $\theta$ .]        | 0.0000           |
| Divergence Slit Type          | Fixed            |
| Divergence Slit Size [°]      | 0.9570           |
| Specimen Length [mm]          | 10.00            |
| Measurement Temperature [°C]  | 25.00            |
| Anode Material                | Cu               |
| K-Alpha1 [Å]                  | 1.54060          |
| K-Alpha2 [Å]                  | 1.54443          |
| K-Beta [Å]                    | 1.39225          |
| K-A2 / K-A1 Ratio             | 0.50000          |
| Generator Settings            | 40 mA, 45 kV     |
| Diffractometer Type           | 0000000011023505 |
| Diffractometer Number         | 0                |
| Goniometer Radius [mm]        | 240.00           |
| Dist. Focus-Diverg. Slit [mm] | 91.00            |
| Incident Beam Monochromator   | No               |
| Spinning                      | No               |

**Main Graphics, Analyze View:** (*Bookmark 2*)

**Peak List:** (*Bookmark 3*)

---

| Pos. [ $^{\circ}2\theta$ .] | FWHM<br>[ $^{\circ}2\theta$ .] | d-spacing<br>[ $\text{\AA}$ ] | Rel. Int. [%] | Area<br>[cts* $^{\circ}2\theta$ .] |
|-----------------------------|--------------------------------|-------------------------------|---------------|------------------------------------|
| 18.3415                     | 0.3346                         | 4.83718                       | 23.03         | 16.97                              |
| 20.3299                     | 0.3346                         | 4.36834                       | 18.57         | 13.68                              |
| 25.5897                     | 0.1506                         | 3.48115                       | 76.56         | 25.39                              |
| 35.1567                     | 0.1840                         | 2.55269                       | 100.00        | 40.54                              |
| 37.7988                     | 0.1506                         | 2.38011                       | 54.13         | 17.96                              |
| 43.3601                     | 0.2342                         | 2.08687                       | 96.90         | 50.00                              |
| 45.5745                     | 0.4684                         | 1.99049                       | 38.28         | 39.50                              |
| 52.5742                     | 0.1673                         | 1.74078                       | 38.85         | 14.32                              |
| 57.5075                     | 0.1673                         | 1.60263                       | 74.61         | 27.50                              |
| 66.5432                     | 0.2676                         | 1.40526                       | 71.05         | 41.90                              |
| 68.2521                     | 0.2856                         | 1.37304                       | 44.33         | 37.70                              |

---



